Review of terahertz and subterahertz wireless communications

Cite as: J. Appl. Phys. **107**, 111101 (2010); https://doi.org/10.1063/1.3386413
Submitted: 04 November 2009 . Accepted: 09 March 2010 . Published Online: 09 June 2010

John Federici, and Lothar Moeller

APPLIED PHYSICS REVIEWS—FOCUSED REVIEW

Review of terahertz and subterahertz wireless communications

John Federici[1,a)] and Lothar Moeller[2,b)]
[1]*Department of Physics, New Jersey Institute of Technology, Newark, New Jersey, 07102 USA*
[2]*Bell Labs, Alcatel-Lucent, Holmdel, New Jersey 07733, USA*

(Received 4 November 2009; accepted 9 March 2010; published online 9 June 2010)

According to Edholm's law, the demand for point-to-point bandwidth in wireless short-range communications has doubled every 18 months over the last 25 years. It can be predicted that data rates of around 5–10 Gb/s will be required in ten years. In order to achieve 10 Gb/s data rates, the carrier frequencies need to be increased beyond 100 GHz. Over the past ten years, several groups have considered the prospects of using sub-terahertz (THz) and THz waves (100–2000 GHz) as a means to transmit data wirelessly. Some of the reported advantages of THz communications links are inherently higher bandwidth compared to millimeter wave links, less susceptibility to scintillation effects than infrared wireless links, and the ability to use THz links for secure communications. Our goal of this paper is to provide a comprehensive review of wireless sub-THz and THz communications. © *2010 American Institute of Physics*. [doi:10.1063/1.3386413]

TABLE OF CONTENTS

I. OVERVIEW OF REVIEW: ADVANTAGES OF TERAHERTZ COMMUNICATION SYSTEMS

The field of terahertz (THz) spectroscopy, imaging, and technology has grown dramatically over the past fifteen years.[1] In conjunction with new and improved THz sources and detectors,[2–7] THz spectrometers and imaging systems[8] have become routine laboratory instruments and have found several niche and industrial applications including explosive and concealed weapon detection,[9–12] pharmaceutical quality control,[13] biology/medicine,[14] and nondestructive evaluation/quality control.[15–17] Over the past ten years, several groups have considered the prospects of using THz waves as a means to transmit data. Numerous papers covering various aspects of the topic—THz sources and detectors, modulation schemes, wireless communication measurements—have been reported in the literature. We comprehensively review approaches to wireless THz communication.

In the literature, there are various definitions of the THz frequency range. For the purposes of this paper, we shall define the sub-THz region as covering 0.1–0.3 THz and the THz region as covering 0.3–10 THz. For the sake of brevity in the paper, we shall use the term "THz" to generically refer to the 0.1–10 THz range, unless otherwise specified. Data

a)Electronic mail: federici@adm.njit.edu. Phone: 973-596-8482.
b)Electronic mail: lmoeller@alcatel-lucent.com. Phone: 732-888-7237.

communication systems that operate, for example, at 94 GHz and below will not be covered by this review unless they directly related to data communications in the sub-THz or THz range. We further limit the review of the field to include THz waves as the free-space carrier of data.

Commercial wireless point-to-point microwave communications systems currently operate at carrier frequencies as high as 18 to 30 GHz (K band and Ka band). Several research projects in the fields of electronics and fiber optics have focused in the past on developing devices for communication system running at 60 GHz signals. The high oxygen absorption peak in this frequency bands strongly attenuates radio signals allowing the design of low interference picocell mobile communication systems with ultrahigh capacity.[18,19] Even at higher frequencies up to 300 GHz the Federal Communications Commission (FCC) has started to allocate frequency bands for mobile, satellite, and wireless links.[20]

Historically, individual (point-to-point) and aggregated (within a volume of space) bandwidth demands for wireless networking have increased rapidly over the last two decades. One way of meeting these bandwidth demands is to increase the spectral utilization efficiency by applying advanced modulation techniques, which enable increased point-to-point data rates, enhanced sharing of a given band of frequencies, and higher amounts of frequency reuse within a volume of space. However, Shannon's channel capacity formula, even when extended to wireless networking in a shared volume of space through the use of multi-input/multioutput approaches, shows an upper limit for this strategy. Beyond this point transmission bands at higher carrier frequencies have to be accessed to provide sufficient transmission capacity. According to Edholm's law of bandwidth,[21] the demand for bandwidth in wireless short-range communications has doubled every 18 months over the last 25 years. (e.g., from less than 1 kb/s for wireless telemetry in 1984 to more than 100 Mb/s with 802.11n wireless local area networks in 2009.) From this recent trend, it can be predicted that data rates of around 5–10 Gb/s will be required in ten years. A review by Koch[22] in 2007 suggests that THz based communications systems will replace or supplement Wireless LAN systems in 2017–2023. Bluetooth and wireless LAN operate at carrier frequencies of only a few gigahertz, so their bandwidth is limited.[22] Even ultra-wide bandwidth technology for indoor communications is only expected to achieve data rates of only 110–200 Mb/s for standard distance and 500 Mb/s at reduced distances.[23]

In the latest United States Federal Strategic Spectrum Plan,[24] it is recognized that Federal agencies universally have an increased demand for higher data throughput and bandwidth—in particular for wireless broadband applications. "These requirements may mean wider operating bandwidths and/or spectrum access in higher frequency bands although most requirements for mobile communications focus on use of spectrum below 5 GHz." It is interesting to note that in the section of the report discussing future federal spectrum requirements above 30 GHz, THz communication is not mentioned as an emerging application. The 30–300 GHz (or EHF) portion of the spectrum is anticipated to be used for radiolocation (radar) service, in particular near 35, 90, 140, and 240 GHz for which there are atmospheric windows for transmission. Above 300 GHz, the frequencies are not allocated currently but probably will be in the future. The main applications envisioned are radio astronomy and remote sensing, not communications. According to this report, the National Science Foundation believes that new allocations in the 0.275 to 1 THz region may be needed within a decade for radio astronomy and other science services. Currently, the main thrust is to use the higher frequency bands (275–2400 GHz) for radio astronomy research. It is anticipated that as research and development applications above 300 GHz emerge, the spectrum requirements will be updated, and frequency bands allocated.

An increasing demand for wireless service equates to a desire for more bandwidth and consequently an implied increase in carrier frequency for communications and data transfers. However, as will be discussed in subsequent sections, in conjunction with the high bandwidth potential, THz wireless links will exhibit an intrinsically short path length and line-of-sight communication. In his discussion of future THz communication systems, Mann[25] considers these limitations and suggests that the commercial application of THz communication links would be a niche in which very high data rates are required over short distances on a multipoint to point/multipoint basis (i.e., the "first" and "last mile" problem). For example, fast dedicated internet access for users in cities where the cost of laying optical cables is prohibitively high is one possible application. Mann further suggests that the compact nature of THz system would allow it to comply with strict planning regulations in cities. THz communication systems with gigabit or higher data rates could enable a wide variety of high bandwidth applications including[26] wireless extensions of broadband access fiber optical networks, wireless extension of high-speed wired local networks,[27] a wireless bridge between lower data rate wireless local networks and high speed fiber-optical networks, high-definition television (HDTV),[28] and broadband indoor picocells to handle high demand from a number of mobile users.

In addition to the intrinsic advantage of potentially ultra-high bandwidth in THz communication links, several other advantages or general properties of THz communication links have been identified in the literature. In some instances, THz wireless communication links offer some advantage over microwave links as well as free-space infrared (IR) based systems. Below is a summary:

- THz communications have the potential for increased bandwidth capacity compared to microwave systems.
- THz communications are inherently more directional than microwave or millimeter (MMW) links due to less free-space diffraction of the waves. A detailed analysis of the link budget[29] estimates that a 10% bandwidth for a 350 GHz link would require antenna gains of 22 dB, 27 dB, 30 dB, and 33 dB for link distances of 1 m, 3 m, 5 m, and 10 m, respectively. The large gain per antenna requires the THz emission to be highly directional and, therefore, line of sight detection is required.
- THz communications can be implemented as a "se-

cure" communications link. THz can support ultrahigh bandwidth spread spectrum systems, which can enable secure communication, large capacity networks, and protection against channel jamming attacks.[30] This topic will be discussed in Sec. III.

- There is lower attenuation of THz radiation compared to IR under certain atmospheric conditions (e.g., fog). Under certain weather conditions and for specific link length requirements THz can enable reliable communication where IR based systems would fail.
- Time varying fluctuations in the real refractive index of the atmospheric path leads to scintillation effects in wireless communications. For THz radiation, these scintillation effects are smaller than for IR radiation allowing THz to provide longer links compared to wireless IR.
- THz communication links are a viable solution for the last mile and first mile problem.[26,31] The last and first mile problem refers to establishing broadbanded, multiuser local wireless connections to high speed networks (i.e., fiber-optical). As an example, THz wireless links could be used as part of the last mile transmission of multiple channel HDTV signals.[27]
- The THz frequency range is largely unregulated.[22] In the United States, 275–300 GHz is reserved[32] for mobile communications. In Europe, above 275 GHz is available for communications.

Communications systems using THz waves, due to the inherently higher bandwidth with increased frequencies compared to microwave systems are an excellent candidate to meet the demand for higher bandwidths. However, there have been relatively few studies of either analog or digital data transmission using THz radiation to date. This in part is due to the fact that the required compact components for communication systems (like planar integrated circuits, amplifiers and antenna arrays) do not exist above 125 GHz. Yet recent technological progress in key technologies such as SiGe, BiCMMOS, and InP suggests that they might be available in a few years from now.[29] Simple components like integrated voltage controlled oscillators were demonstrated by Bell Laboratories in InP HBT technology with output power of -10 dBm at 350 GHz. Recently, integrated millimeter wave integrated circuit (MMIC) chip sets have been developed at 125 GHz and utilized in a 10 Gb/s 800 m long wireless link.[33] Likely, fully electronic THz communications systems running at carrier frequencies of a few 100 GHz will become reality in the near future when sufficiently fast and powerful integrated circuit electronics are available. Consequently, most of the THz communications measurements done to date have used alternative hardware (such as THz time-domain systems, microwave mixers, etc.). Studies of THz communications issues have largely focused on items such as indoor and outdoor channel modeling, study of propagation effects, evaluation of modulation schemes, and THz hardware components.

The intrinsic advantage of THz communication systems compared to microwave or millimeter wave systems is that of higher bandwidth. However, what about the other competing frequency range, namely free-space IR communications? IR free space communication links at 1.5 μm wavelength are the most common optical transmission vehicle for short reach (up to 10 km). As previously noted by Koch,[22] wireless IR systems are 30 years old, yet the highest data rates reported are 155 Mb/s.[34] A 2007 review of the field in Ref. 35 shows no improvement beyond the 155 Mb/s data rate reported in 2001. Only recently has a 10 Gb/s data rate been demonstrated in a simulated atmospheric environment.[36] The key to increasing the IR wireless data rate to 10 Gb/s was advanced modulation formats such as orthogonal frequency division multiplexing. Coherence detection and multiple input multiple output (MIMO) processing as been used to demonstrate a 100 Gb/s per channel link.[109]

Two of the most important issues with IR free-space communications are transceiver misalignment due to atmospheric turbulence and/or humidity fluctuations in the beam path (i.e., scintillation) as well as atmospheric absorbance of the IR signal.[37] Atmospheric turbulence and humidity fluctuations cause temporally and spatially dependence variations in the atmospheric real refractive index. Consequently, the location of the IR beam on the receiver tends to vary in time leading to scintillation effects. This effect will be discussed in Sec. II. Another possible advantage of THz compared to IR communication systems that has been identified[22] is that intensity modulation and detection with IR photodetectors is not as sensitive as THz heterodyne detectors. Moreover, there is more ambient IR light noise typically present compared to ambient THz noise. Lastly, there is an eye safety issue with IR wavelengths requiring that the IR transmitted power be limited to eye-safe power levels.

II. THZ AND SUB-THZ COMMUNICATIONS: BASIC CONSIDERATIONS

In this section, basic considerations of THz and sub-THz communication are discussed including

- Free space versus guided waves.
- Directionality.
- Scintillations.
- Atmospheric and free-space damping including fog, rain, and dust/smoke.
- Indoor versus outdoor communication.

A. Free space propagation versus guided THz waves

Unlike the near-IR wavelengths for which low loss optical fibers are available, THz fibers (such as bare metal wires,[38] hollow-glass metallic waveguides,[39] and photonic crystal fibers[40]) are characterized by a fairly sizeable attenuation: typically in the 0.01–0.03 cm^{-1} range. Therefore, it is unlikely that THz communication systems will utilized THz fibers for propagation over long distances since fiber optical communication systems can carry very high data rates >100 Gb/s over long (tens of kilometer) distances. For short distance transmission less than a meter (for example, through a barrier such as a wall), THz fibers might be preferable to the intrinsic attenuation and scattering by building material. However, for longer distances through a building,

the radio-over-fiber (RoF) method (described in Sec. VI) can use optical fibers to deliver THz modulated optical signals to the exterior of buildings before converting to free space THz radiation. As THz sources and detectors are developed for communication, THz waveguides may fill a critical role in the coupling of radiation between THz components.

B. Directionality of THz radiation

The importance of the diffractive effects in free-space THz systems can be explored using the Friis formula. Following the analysis of Brown,[41] the power supplied to the load of the receiving antenna is given by

$$P_{\text{out}} = P_{\text{in}}\left(\frac{\lambda}{4\pi d}\right)^2 G_r G_t F_r(\theta_r,\phi_r) F_t(\theta_t,\phi_t)\tau\varepsilon_p, \tag{1}$$

where P_{in} is the input power to the transmitting antenna, G is the antenna gain, F is the normalized intensity pattern function, τ is the path power transmission factor, ε_p is the polarization coupling efficiency, λ is the wavelength of the radiation, and d is the distance between the transmitting (t) and receiving (r) antenna. The angles θ and ϕ refer to spherical coordinates at either the receiver or transmitter. The free-space loss factor $(\lambda/4\pi d)^2$ arises from two effects: (1) The assumption that the receiving antenna is detecting the far-field radiation of the transmitting antenna leads to treating the source as emitting a spherical-like wave whose power decreases as $1/d^2$ with distance. (2) The factor of λ^2 arises from the diffraction limited directivity (D_{max}) or alternatively the solid angle which defines the extent of the diffracting intensity pattern function such as: $D_{\text{max}}=4\pi/\Omega=4\pi A_{\text{eff}}/\lambda^2$, for which A_{eff} is the effective area of the detector.

The antenna gain and directivity are related by

$$G_t = \frac{P_{\text{rad}}}{P_{\text{in}}} D_t, \tag{2}$$

where P_{rad} is the power radiated by the antenna. If we assume that the radiation and input powers are matched, then the gain of the antenna is equal to the directivity. In this case, Eq. (1) can be rewritten as

$$P_{\text{out}} = P_{\text{in}} \frac{A_t A_r}{d^2\lambda^2} F_r(\theta_r,\phi_r) F_t(\theta_t,\phi_t)\tau\varepsilon_p, \tag{3}$$

where A_t and A_r refer to the effective areas of the transmitter and receiver, respectively. According to Eq. (3), the power received at a detector varies as $1/\lambda^2$ so the efficiency of detection improves as the wavelength decreases or the THz frequency increases. This implies that THz communications are inherently more directional than microwave or MMW links due to less free-space diffraction of the waves. Consequently, THz communication systems will typically be line-of-sight systems.

Mann[25] used a simplified version of Eq. (3) to estimate the maximum data transmission distance of a 400 GHz versus a 60 GHz system. Despite the fact that THz sources are currently less powerful than comparably sized microwave sources, the maximum distances for data transmission (~1.9–2.0 km) are comparable. The low power of a 400 GHz system is compensated by the fact that the 400 GHz radiation diffracts less than 60 GHz radiation.

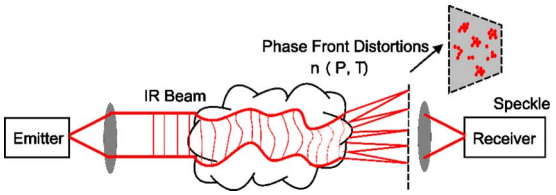

FIG. 1. (Color online) Air turbulence causes refractive index fluctuations resulting into speckle (intensity variations at receiver) that limits the reach of IR systems.

C. Scintillation

Real refractive index fluctuations can destroy the flat phase front of an IR light beam when it passes a few kilometers of air. Local temperature, pressure, or humidity gradients, which are generated by thermals and turbulences near ground level, cause small refractive index variations across the wave front of the beam. Even if a single local refractive index fluctuation only slightly distorts the wave's phase front, the effect can accumulate over a few kilometers of propagation distance resulting into a complete or almost complete destruction of the phase front. As a consequence, on the receiver side the beam cross section appears as a speckle pattern (Fig. 1) with huge local and temporal intensity variations preventing detection of constantly sufficient signal power. In the absence of fog, these scintillation effects are the main link length limitation in free-space IR communication systems. Complex equalizer schemes for phase front correction based on mirrors arrays were proposed as counter measure but could not show so far convincing performance. As will be discussed below, THz beams are much less susceptibly to scintillation compared to IR beams.

The refraction index of air in the millimeter wave band up to a few hundred gigahertz can be well approximated as function of temperature and pressure by

$$n_{\text{mmW}} \approx 1 + \frac{7.76}{T}\left[P_a + 4810\frac{P_{\text{v}}}{T}\right] \times 10^{-6}, \tag{4}$$

where T, P_a, P_{v} stand for the temperature in kelvin, the atmospheric pressure in kilopascal, and the water vapor pressure in kilopascal, respectively.[42] Similarly, for IR wavelengths the refraction index of air can be written as:

$$n_{\text{IR}} \approx 1 + 7.76\times 10^{-6}[1 + 7.52\times 10^{-3}\lambda^{-2}]\frac{P_a}{T}$$

$$\cong 1 + 7.76\times 10^{-6}\frac{P_a}{T}, \tag{5}$$

where λ stands for the wavelength in micrometers.[43] The formula does not consider humidity as it only insignificantly degrades IR propagation. Under the assumption of relevant air parameters a numerical comparison of both formulas shows that even at high levels of water vapor pressure the

refraction index changes in both the THz and IR bands are comparable. Since scintillation effects are driven by variations in phase, the relevant parameter is the variation in the optical path length relative to the electromagnetic wavelength. Since the variation in the optical path length for both the IR and THz are comparable (the changes in refractive index are commensurate), the relative magnitudes of the phase variations are predominately determined by the electromagnetic wavelength. The wavelength of THz at ~200 GHz is approximately 1000 times longer than the wavelength of 1.5 μm light. Consequently, scintillation and speckle effects in the THz beam are expected to be significantly smaller than in the IR.

There have been some measurements of scintillation effects at 97 GHz which showed that the long-term probability distribution of scintillation amplitudes could be modeled by the Mousley–Vilar equation.[44] Knowledge of the scintillation amplitude distribution can be used to predict the degradation of the communication link due to scintillation. The only experimental evidence that has been published concerning the effect of scintillation on THz communication is a brief comment in Ref. 33. That paper describes the effect of wind on the THz communication measurements at 125 GHz. As wind velocity increases, the lateral deviation of the THz beam from the receiver axis also increases which caused the input power to the receiver to decrease. However, since the detected power was greater than the minimum required, the authors did not observe any increase in bit-error-ratio.

D. Atmospheric and free-space damping including fog, rain, and snow

Atmospheric attenuation of THz and IR communications are impacted differently by weather conditions such as fog, rain, snow, and humidity. Figure 2 compares the absorption coefficient of millimeter waves, THz, and IR waves at sea level for different weather conditions. Under fog conditions the THz absorption at ~240 GHz is around 8 dB/km which is considerably lower than the 200 dB/km that the 1.5 μm wavelength suffers. The maximum reach of THz radiation in fog can be much larger than those of usual IR based systems. Thus T-rays based communication systems could serve as a back-up for foggy weather when IR signaling fails. It also should be noted that above 200 GHz and below 10 THz, the attenuation is dominated by atmospheric water vapor, with attenuation due to rain and fog playing a minor role. In the IR, fog and smoke will cause significant attenuation. As noted by Brown[41] in his extensive consideration of MMW

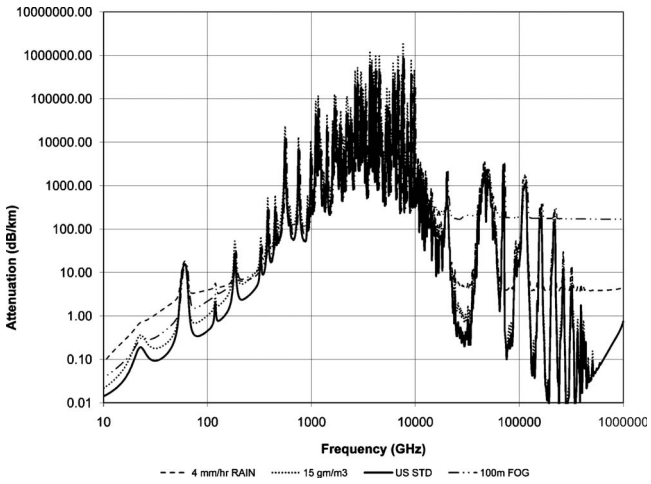

FIG. 2. Calculated atmospheric attenuation in THz and IR band. ITU recommendations are used from 10 to 1000 GHz. MODTRAN 4 is used from 30 to 0.3 μm. A code for the 1–10 THz region was developed by MMW Concepts LLL (Ref. 45). The dashed line corresponds to 4 mm/h of rain. The dash-dot line corresponds to 100 m visibility of fog, and the solid line corresponds to U.S. standard atmospheric conditions at sea level (59% relative humidity=7.5 g/m^3 water content). The dotted line corresponds to 15 g/m^3 of water content. A wavelength of 1.5 μm corresponds to 2×10^5 GHz.

and THz remote sensing systems, there is little or no experimental data on THz scattering by fog, rain, particulates, etc. Brown attributes the limited experimental data to a lack of calibrated THz instrumentation and the general difficulty in distinguishing absorption from scattering effects. While experimental data at 97 GHz (Ref. 44) indicates a reasonable agreement between measured rain attenuation values and those predicted by different models, differences in the measured and predicted values suggest that further measurements are required to fully validate rain attenuation models at the higher MMW or sub-THz frequency range.

Due to the relatively small size of atmospheric particulates such as dust and smoke compared to the THz wavelength, one would expect minimal THz attenuation due to airborne particulates. Mann had predicted that fog and smoke has little or no effect up to 1 THz.[25] A rough estimate of the attenuation can be made assuming that the particulates act as spherical Mie scattering centers. Following a simple Mie scattering formalism[46] that was used previously to study attenuation of THz radiation due to particle grains,[47] one can estimate the attenuation at IR, THz, and sub-THz frequencies using known particles sizes and concentrations. The extinction coefficient takes on the following form

$$\mu_{\mathrm{th}}(\nu) = N\frac{c^2}{2\pi\nu^2}\sum_{m=1}^{\infty}(2m+1)\mathrm{Re}(a_m + b_m), \tag{6}$$

where N is the number of particles per unit volume, c is the speed of light, ν is the electromagnetic frequency, Re denotes real part, and a_m and b_m are the coefficients in the infinite summation such that,

$$\begin{cases} a_m = \dfrac{\psi_m'(y)\psi_m(x) - n\psi_m(y)\psi_m'(x)}{\psi_m'(y)\zeta_m(x) - n\psi_m(y)\zeta_m'(x)} \\ b_m = \dfrac{n\psi_m'(y)\psi_m(x) - \psi_m(y)\psi_m'(x)}{n\psi_m'(y)\zeta_m(x) - \psi_m(y)\zeta_m'(x)} \end{cases} \quad \text{where} \quad \begin{cases} \psi_m(z) = zj_m(z) \\ \zeta_m(z) = zh_m^{(2)}(z) \end{cases} . \tag{7}$$

Here $j_m(z)$ and $h_m^{(2)}(z)$ are spherical Bessel functions of the first kind and third kind, respectively. The parameter z can be either $x=2\pi\nu r/c$ or $y=2\pi\nu nr/c$, where r is the radius of the spherical particle and n is the frequency independent refractive index of the particle.

As an example, we can estimate the attenuation due to battlefield[48] or wildfire particulates and smoke[49] using Eqs. (6) and (7). As shown in Fig. 3, IR wavelengths are strongly attenuated while THz and sub-THz wavelengths would enable communications through a much longer link distance.

The attenuation of THz radiation is a function of altitude and temperature. At higher altitudes, the humidity decreases leading to a large increase in the maximum distance for THz communication. Figure 4 illustrates the predicted channel capacity as a function of frequency for a link from the ground to an unmanned aerial vehicle at 5 km altitude.[50] The model assumes a linear channel which is distorted by white Gaussian noise and atmospheric absorption. It calculates the channel capacity based on the Shannon–Hartley theorem and the system parameters shown in the legend of Fig. 4. We compare three cases such as: (a) the channel bandwidth is fixed at 100 MHz (dotted curve) and (b) the channel bandwidths equals 10% of the carrier frequency (solid curve). In both cases we assume signal propagation under vacuum conditions (no absorption). To visualize the atmospheric effects on the communication link, we assume in case (c) the channel bandwidth to be again 10% of the carrier frequency but also moderate rain with 4 mm/h precipitation across the signal propagation path. Due to strong attenuation at higher THz frequencies, the effective channel capacity is reduced. Above about 500 GHz the channel capacity drops sharply about five orders of magnitude. From this we can conclude that ultrahigh capacity channels (>10 Gb/s) with transmission distances of over several kilometers have to operate in the frequency range between approximately 100 and 300 GHz.

As an example of how humidity and other weather conditions effect THz communication, we theoretically consider[51] a communication link operating around 250 GHz (Fig. 5). As illustrated in the figure inset, 250 GHz is chosen because it is roughly in the middle of the 200–300 GHz atmospheric transmission window. A 100 Gb/s differential phase-shift keying signal is encoded on the 250 GHz carrier on the transmitter side by means of a Mach–Zehnder modulator (MZM), driving in push-pull operation. The sub-THz signal propagates through a channel whose water content can be varied. The inlay in Fig. 5 shows qualitatively the impact of humidity on the transmission band. Clearly, the channel attenuation increases but also the passband is tilted with increasing water content. The resulting bandwidth limitation causes significant distortions which we visualize by simulating the baseband eye diagram of the received signal. The baseband signal is generated by down mixing the received signal and launching it through a Mach–Zehnder interferometer to convert its phase coding into an amplitude modulation. In the first case, we assume standard weather conditions and plot (Fig. 6) the eye diagram for back-to-back, 1, 2, and 3 km transmission distances. To highlight the impairment by channel bandwidth reduction, we normalize the received signal power (no attenuation by absorption). After about 3 km the eye diagram is completely closed preventing high quality data communication. In the second case (Fig. 5) we assume rain at a rate of 4 mm/h across the free space propagation area. As expected the impairments are even stronger than in

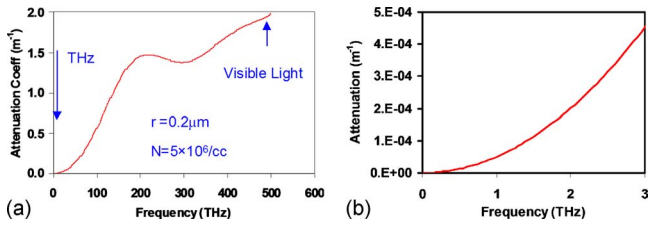

FIG. 3. (Color online) Predicted IR (a), THz, and sub-THz (b) attenuation due to spherical airborne particles. For the calculation, parameters comparable to battlefield fog oil particles are used: particle density 5×10^6/cc, 0.2 μm particle radius, and a real index of 1.5.

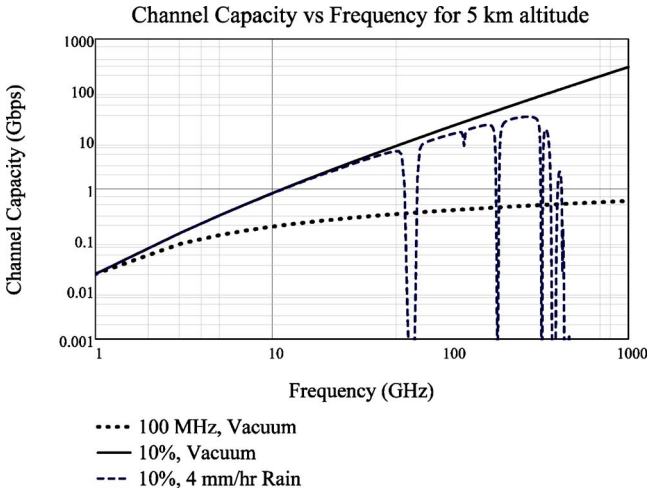

FIG. 4. (Color online) Channel capacity vs frequency for a link between the ground and an airborne vehicle at 5 km altitude. The communications channel follows a line of sight path from the ground to the vehicle at an angle of 30° relative to the horizontal. The dotted line corresponds to a fixed bandwidth of 100 MHz, the solid line corresponds to a 10% bandwidth in vacuum, while the dashed line corresponds to 10% bandwidth in rain at a rate of 4 mm/h. For this calculation, the transmitter power is assumed to be 0.5 W. The diameter of both the transmitter and receiver antennas is 7.5 cm, the noise figure is 8 dB, and the antenna loss is 3 dB.

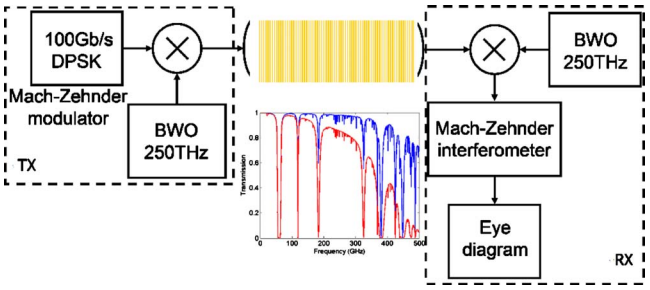

FIG. 5. (Color online) Simulating distortions to eye diagrams from atmospheric attenuation.

the case of standard weather conditions. The eye diagram is already completely closed after 2 km transmission. This simulation shows that weather conditions have to be considered during the system design. To mitigate eye distortions, it could be better to split the 100 Gb/s data load onto ten channels (each at 10 Gb/s) which are frequency spaced. Other alternatives could be to apply more bandwidth efficient modulation formats e.g., quadrature phase-shift keying or signal equalization on the receiver side.

E. Indoor versus outdoor

In considering the atmospheric attenuation of THz waves, clearly certain spectral "windows" are available for THz communication such as the 200–300 GHz window of Fig. 2. Based on the strong atmospheric attenuation, Koch[22] concludes that practical THz communication distances are limited to several tens of meters. Therefore, he predicts that THz wireless systems will be limited to medium-link and short link *indoor* applications since outdoor scenarios are much less likely unless adverse weather conditions are rare. Since both indoor and outdoor THz systems exhibit smaller diffractive effects at THz frequencies compared to microwave frequencies, one would expect that any THz system would require line of sight connection between transmitter and receiver. For outdoor systems, this restriction is less of a problem, for example, if the transmitter and receivers were placed on roof-tops of buildings. For indoor systems, one would have to rely on nonline of sight paths including reflections from walls. Clearly objects or people moving in the beam path will severely disrupt the communication channel.

Using the Friis equation, a simple estimation for a reliable indoor THz link suggests that 31 dB gain per antenna is needed to compensate for free space damping.[22] A more detailed analysis of the link budget[29] estimates that a 10% bandwidth for a 350 GHz THz link would require antenna gains of 22 dB, 27 dB, 30 dB, and 33 dB for link distances of 1 m, 3 m, 5 m, and 10 m, respectively. The large gain per antenna requires the THz emission to be highly directional and therefore line of sight detection is required. It is important to note that this modality of a THz wireless data link is very different from today's indoor wireless communication systems. Consequently, implementation of an indoor link THz communication cannot be just an extension of existing technology but must involves the development of new concepts and ideas to make it feasible.[22]

As a further example of the need for new ideas, objects can block line of sight (people moving around in a room) so that alternative nonline of sight routes, such as reflections from walls, are required for a THz communications link. However, since the reflection from typically building materials[52] would introduce additional losses in the links, highly reflecting mirrors are needed. In addition, steerable high-gain antennas are required to connect from another path in case the primary path is blocked.

A key hardware component to implementing indoor THz communications is reflective "wall paper" that increases the THz reflection[53] from walls in the event of a nonline of sight path in a room. The first version of the reflecting paper[54] used alternating layers of plastics (real refractive indices 1.7 and 1.59). Stacked alternative layers produced a relatively high reflectivity (76%) at 187 GHz with a ~16 GHz bandwidth. One advantage of these dielectric mirrors is that they are flexible since they can be fabricated with flexible plastics. However, the maximum reflectivity is limited by the index difference between the different layers. An improved version of the mirrors, described in Ref. 55, consists of alternating stacks of polypropylene ($n=1.53$) and high resistivity silicon ($n=3.418$). These mirrors, due to the large index difference between adjacent layers, have high reflectivity (>95%) for both *s*-polarization and *p*-polarization regardless of incident angle. The bandwidth of the mirrors is limited to ~56 GHz due to the shifting of the *p*-polarization reflection band with incident angle. Measurements of the dispersive properties of the mirror show that the group delay is on the order of a 5 ps (Ref. 56) with some variation in both the THz frequency (between 0.25 and 0.4 THz) and polarization. Unfortunately, the 63 μm thick crystalline silicon layers are not flexible. However, a flexible high-index dielectric could be fabricated by mixing high resistivity silicon or TiO_2 powder with polypropylene and coextruded.[57] This should improve both the quality and uniformity of a flexible dielectric THz mirror.

In order to characterize the indoor THz communication channel, ray tracing, and Monte Carlo simulations were performed.[22] Ray tracing techniques can be used since the THz wavelength is small compared to the geometric size of typical indoor scatterers. Consequently, the THz communication channel can be described using basic parameters such as free-space attenuation, reflection coefficients from objects in the room, antenna gains, and the power delay profile. The power delay profile refers to the path length difference between the direct line of sight and once or twice reflected THz radiation. Clearly, there will be a time delay in the data at the receiving antenna depending of which path is taken. If the data rate were too high, there would be intersymbol interference (ISI) between data traveling along the multiple paths.

In the simulation environment, models are included for people and objects. They are placed randomly in a "cell" or room and geometrically modeled with planes of appropriate dimensions and THz reflectivity. People are considered to be totally absorbing. Metallic surfaces are considered to reflect THz radiation perfectly. Reflection of smooth objects are modeled with Fresnel equations using the known complex indices of refraction and angles of incidence as input data. In some of the earlier simulations, it was shown that high gain

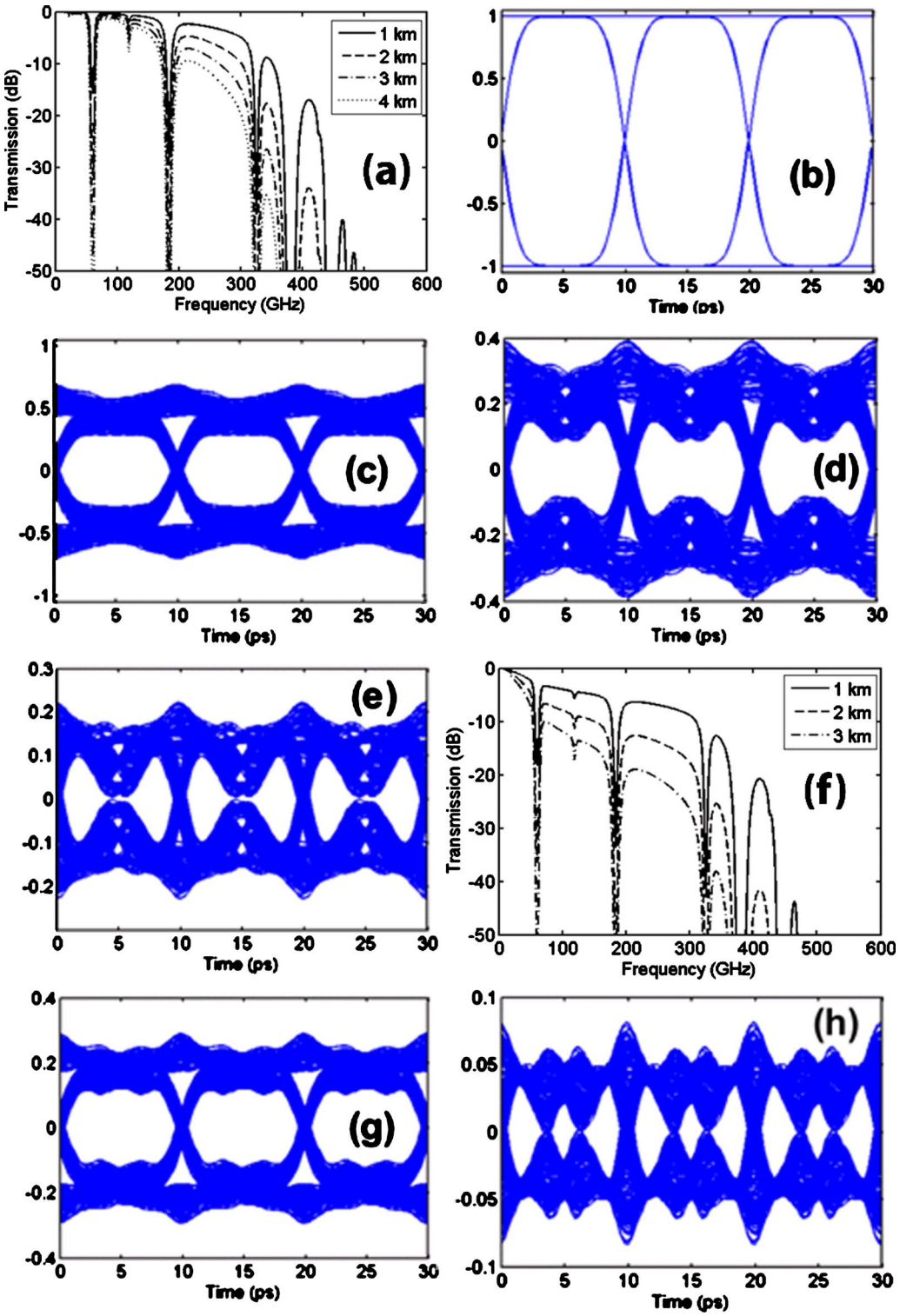

FIG. 6. (Color online) (a) Simulated transmission bands as a function of frequency and link distance for standard weather conditions. Simulated eye diagrams for transmission distances of (b) 0 km, (c) 1 km, (d) 2 km, and (e) 3 km. Equivalent transmission (f) and eye diagrams for rain at a rate of 4 mm/h at link distances of (g) 1 km and (h) 2 km.

antennas are required for indoor THz communication links. In addition, the placement of people was considered to be static. The simulations have been improved[26] to consider motion of people including their speed movement, direction of motion, and changes in direction of motion. The simulation allows people to be moving in the room for 30 s. The THz transmitter is positioned on the ceiling while the receiver is located on a desktop in the room. Monte Carlo ray tracing from transmitter to receiver establishes THz communication channel statistical properties.

The simulation calculates the THz power at the receiver from direct line of site paths, once reflected paths, and twice reflected paths. The assumed sensitivity limit for detection is −110 dBm. 30% of all simulated paths are interrupted by

interfering objects. Shadowing effects are observed predominately near static objects such as furniture and walls. While direct line of sight is not feasible due to moving objects, twice reflected power should be avoided: more than −100 dBm of power from twice reflected path is available only 30% of time. Once reflected paths provide more than −95 dBm of the power 65% of the time. Consequently, the indoor link design should depend on direct line of sight power and once reflected light.

If the data rate were too high, there would be ISI between the multiple paths. Consequently, the data rate must be slow enough to eliminate ISI. For the simulated channels, 90% have a time delay spread of less then 10 ns. From this maximum time delay, Piesiewicz *et al.*[26] estimate a maximum data rate of 5 Mb/s on a given binary channel. Multiple channels would be required to achieve gigabit per second data rates. Since the THz beams are highly directional, Piesiewicz *et al.* suggest that "smart" (steerable) antennas could utilize one propagation path at a time and therefore eliminate ISI. However, such an antenna system still needs to be developed and evaluated.

In summary, from these simulations it is concluded that (a) alternative routes are needed in which THz reflects off of walls to make the system robust against obstacles blocking a primary line-of-sight path of the THz beam. Only direct line of sight and once reflected beams should be utilized, (b) dielectric mirrors improve indoor THz communications by increasing the reflectivity of the walls for nonline of sight links, and (c) interference (ISI) among the various beam paths limits the maximum data rate in a single binary channel. Multiple channels are required for gigabit per second data rates. (d) Lastly, high gain and smart steerable THz antennas are needed to switch between different link paths to minimize ISI.

III. SECURE WIRELESS THZ COMMUNICATIONS

Many papers in the THz scientific literature—whether they discuss THz sources, detectors, components, or communication—typically motivate their work by rightfully claiming that THz can be used for "secure" communications. Scenarios for secure links might include stealthy short distance communications between vehicles (manned or unmanned) and personnel. Unmanned vehicles may require short-distance secure communications links so that they can receive instructions/transmit data before dispersing to conduct their remote controlled or autonomous mission. In order for the link to be secure, unauthorized personnel should not be able to identify either the data via eavesdropping on communication channels or the presence of a communication link.

A major driving force within the United States Department of Defense (DOD) for secure wireless THz communications may result from plans[24] for broadband mobile-on-the-move technologies using both terrestrial and satellite units. DOD expects that its requirements beyond 2014 will be driven by a transition to wideband networks. This shift in technology mirrors the DOD's desire to shift from a manual spectrum management plan to an autonomous electromagnetic spectrum management regime. Beyond 2014, DOD's spectrum use will be driven by the transition to wideband network waveform wireless networks that contribute to DOD's network centric warfare model. Through such new technology, DOD plans a combat system that can link ground, maritime, aeronautical, and space operations with layered redundancy, constant connectivity, and situational awareness. Clearly, for such a system high bandwidth and secure communications are essential. As part of a complete system, THz communication links could provide both of these essential features.

What are the characteristics of THz communication that makes it secure? (a) highly directional beams compared to microwave communications, (b) less scattering of radiation compared to IR wireless, (c) limited propagation distance due to atmospheric attenuation, (d) encryption of the beam, (e) large channel bandwidth for spread spectrum techniques which enable antijamming and low probability of detection systems, and (f) hidden THz signals in the background noise.

Since the frequency of THz radiation is larger than that of microwaves, beams of THz radiation will diffract less during free-space propagation. Consequently, as discussed previously, THz communication is typically line-of-sight. Since the THz communication beams are highly directional, it is possible to minimize the area over which THz radiation can be detected. Microwave wireless communication is less directional; the side-lobes of microwave radiation could be more easily detected by unauthorized personnel. On the other extreme of frequency, IR wireless communications are more highly directional than THz due to the higher carrier frequency and smaller potential beam diameter. However, IR radiation is more efficiently scattered by airborne particles. Scattered IR radiation from airborne particles could be detected thereby compromising the communication channel.

Intrinsic atmospheric attenuation of THz radiation, while limiting the maximum distance for wireless communications, could also be a benefit for secure links. Atmospheric absorption controls signal spreading and limits the detection area. Attenuated wavelengths in IR links (5–7 μm) can be used for secure communications.[37] For short distances, data transmission to the intended target detector can be facilitated since the radiation is highly directional. However, the link is secure over longer distances since the radiation is absorbed by the atmosphere. Similarly for THz radiation outside of a limited propagation distance, the THz radiation is highly absorbed by the atmosphere making unwanted detection of data very difficult. The communication of such systems can be limited by absorption to certain geographic areas thus it will be much more difficult to detect and intercept the signals outside of these areas by eavesdropping even when the system is running in a broadcasting mode.

In addition to the intrinsic propagation properties that enable secure THz communication, the technological advantage of an ultrawide-bandwidth communication system can reduce an adversary's chances for successful attacks on a protected link. For example, the large channel bandwidth of THz systems allows for specific protection measures for channels against various standoff attacks like jamming. Another advantage of ultrahigh bandwidth THz systems, in ad-

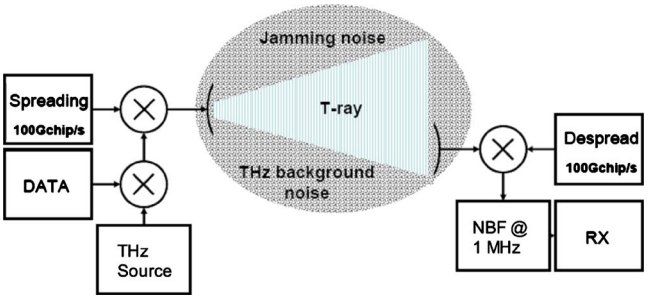

FIG. 7. (Color online) Schematic of hidden THz communication link utilizing ultrawide THz bandwidth. The spreading factor is 10^5 (100 Gb/s:1 Mb/s).

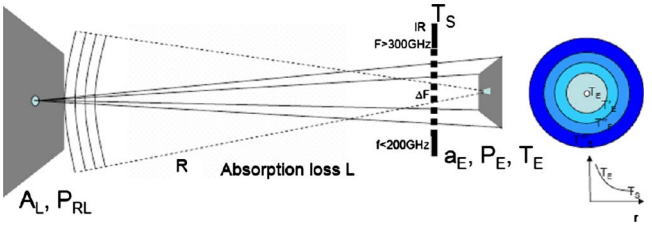

FIG. 8. (Color online) Channel cooling together with spread spectrum techniques result in a spectrally invisible emitter.

dition to immunity against standoff jamming attacks, could be the ability for completely hiding information exchange.

Communication systems can be roughly subdivided into three different categories of security. Well-known are methods for encrypting data using codes thus only a receiver with the right key can decode and read the information. However, this method does not tell the receiver if eavesdropping takes place along the link. Quantum cryptography establishes data exchange based on entangled states of particles. Such schemes indicate to the receiver possible eavesdropping attempts. However, eavesdroppers or other unauthorized third parties will at least be able to notice that data exchange between sender and receiver is on going. We are suggesting a third and novel kind of secure THz communication: an ultrawide bandwidth THz channel allows for low probability of detection communication such that the communication links can be in principle be completely hidden such that a third party would not even notice that signals are exchanged.

The atmospheric THz transmission window with a center frequency around 240 GHz offers about 100 GHz of bandwidth. Spreading the data throughout the 100 GHz bandwidth makes the system difficult to jam because an adversary would need to generate high power to overwhelm the THz receiver. The key to this antijamming technique is to efficiently spread the data throughout the available THz bandwidth using high speed modulators and demodulators. While it will take still some time before ultrawide bandwidth modulators and demodulators for THz signaling are available, technology for designing multiplexers and demultiplexers to perform logic data processing at 100 Gb/s already exists for ultrahigh speed fiber communication at 1.5 μm wavelengths. We explain the operation principle of the frequency spreading system by means of Fig. 7. A 1 Mb/s data signal, modulated on the continuous wave (cw) output of a THz source, is encrypted using a long code sequence at a chip rate of 100 Gb/s. A signal from a jamming attack that does not carry the correct codeword but possesses the right carrier frequency and chip rate will get further spectrally broadened in the decoder by approximately a factor of $\sqrt{2}$ depending on the chosen modulation format. Assuming that the transmitter signal is perfectly deconvoluted and has a spectral efficiency of about 1 bit/s/Hz then narrow bandwidth post filtering at the decoder output results in a rejection ratio for jamming attacks of about 40 dB, i.e., a potential jammer must possess a technology advantage allowing for building sources that output several orders of magnitude more power in order to prevent communication. However, it will probably be extremely challenging to modulate 100 Gb/s data signals on a carrier at 240 GHz due to the required unusually high bandwidth-to-carrier-frequency ratios.

As an example, of the frequency spreading, consider a broadcast configuration in which the THz signal is emitted at a power level of -14 dBm (which can be reached, for example, with an integrated multiplied microwave source), and intensity-wise evenly radiated across an area of 10 km^2 size. A receiver antenna with an effective aperture of 1 m^2 would collect about -104 dBm power. This level is sufficient to detect the data at high quality if the decoding can be assumed to be lossless and a 20 dB link margin can account for atmospheric propagation losses. A 20 dB power margin to compensate for coding and decoding losses can be achieved by increasing the emitter power to about 4 mW.[58] In principle the receiver noise is limited by the thermal noise of the antenna. Thus at room temperature and a signal bandwidth of $\Delta B_{\mathrm{sig}} \sim 1$ MHz, the antenna noise after narrow bandwidth filtering accumulates to $N_o = k_B T\ \Delta B_{\mathrm{sig}} = 4$ fW leading to a signal-to-noise ratio of approximately 10 dB. If a loop finder, used to locate a hidden sender, is steering directly in the direction of the emitter but does not have the right code sequence to decode the signal then it would measure the emitted signal as a slightly enhanced antenna noise. More quantitatively, the detected ultrawide bandwidth signal would appear as an antenna temperature enhancement of $\Delta T \sim -104\ \mathrm{dBm}/(k_B \times 100\ \mathrm{GHz}) \sim 30$ mK.

Although this amount is very small compared to possible natural environmental sources, the signal spectrum could in principle be completely hidden in the thermal noise by using "channel cooling." The idea is sketched in Fig. 8. The aperture of the THz emitter is surrounded by a mounted cooled plate and radiates into the area where a receiver and a possible loop finder is located. It can be shown that if the loop finder were far enough away such that its spatial resolution is not high enough to selectively detect the emitter aperture and the cooled plate, it would measure only an average antenna noise that could be chosen to be adjusted to the environment level. Hence, the emitter would be in its active frequency range spectrally invisible. This example is just intended to illustrate the main idea behind channel cooling for concealing the emitter. The amount of cooling depends on several system parameters like, distance, plate size, received power, apertures of the loop finder and emitter. However, we expect that under assumption of reasonable system parameters a cooling of a few degrees kelvin for a plate with size compa-

rable to the emitter aperture is sufficient to hide the sender. We mention that a more detailed analysis is required to fully describe the potential of this method, e.g., the concept works best if absorption losses in the atmosphere can be neglected.

IV. THZ HARDWARE FOR WIRELESS COMMUNICATIONS

In this section, we will review the basic hardware for THz communications links including methods of THz generation, THz detection, and modulation.

A. Methods of THz generation

1. Optoelectronic

Using optoelectronic generation, one has a variety of options to convert beat frequencies from visible/near IR laser beams to THz signals including via photodetection [e.g., unitraveling-carrier photodiode (UTC-PD), comb frequency generators], cw photomixing, and of course time-domain THz generation. Since optoelectronic THz sources have been recently reviewed,[59] we emphasize the highlights that are relevant for THz communication. In this section, we will focus on THz generation by ultrafast pulsed lasers, rectification in fast PDs (e.g., UTC-PD and optical frequency comb generators), and cw photomixing.

One of the older methods for the generation and detection of THz radiation utilizes photoconductive antenna (PDA) structures. The PDAs are typically fabricated using a fast photoconductive material (for example, low-temperature grown GaAs) which acts as a fast switch in a metallic (e.g., gold) antenna structure. When the unilluminated structure is biased with a constant voltage, no current flows in the device since there are virtually no optical induced charge carriers in the photoconductive switch. Upon illumination with a short optical pulse, for example from a mode-locked Ti:sapphire laser, the photoconductive switch closes (becomes highly conductive), and there is a brief surge of current in the antenna structure. By Maxwell's equations for electromagnetics, the time-varying current induces a freely propagating THz electromagnetic wave. This structure, which is extensively used in THz time-domain spectroscopy (THz-TDS), is well-known[60] and will not be reviewed here. The pulses, which are generated and received by THz emitter and detector modules, possess a bandwidth of roughly 0.1 to 2.5 THz (wavelength range of 0.12 to 3 mm). The technology has been sufficiently developed that photoconductive THz sources and detectors, as well as cw photomixers, are commercially available from companies such as Physical Domains, T-Ray Science, and GigaOptics.

Related to the PDA structure for THz-TDS are cw photomixers for THz radiation.[61,62] In the literature, photomixing is sometimes called optical heterodyne conversion in a photoconductive switch. However, it should be noted that optimizing the photoconductive devices for THz time-domain does not necessarily also optimize the devices for cw photomixing. In the photomixing process, two colinear optical or near-IR beams illuminate the photomixing structure. The two beams are typically narrow optical bandwidth laser sources which are frequency stabilized. For efficient photomixing, the polarizations, frequencies, and phases of the input optical beams must be stable. Similarly (as will be discussed below) a stable pulse repetition rate is important for both THz-TDS and optical frequency comb generation of THz radiation. The photomixing process produces a THz beam at the difference frequency of the two laser beams. The THz frequency is adjusted by tuning the difference frequency of the two IR laser sources. Whereas the time-domain method produces a THz pulse that is spectrally broad, the cw mixing method produces a narrowband THz signal which is typically limited by the linewidth of the lasers to roughly 1–2 MHz.

As pointed out by Duffy *et al.*,[61] photomixing is fundamentally different from second-order $\chi^{(2)}$ nonlinearities which give rise to difference frequency generation. For the $\chi^{(2)}$ processes, two optical photons produce a single low energy THz photon with low quantum efficiency. Consequently, photomixing is more efficient that $\chi^{(2)}$ difference frequency generation at low THz frequencies. At higher THz frequencies, $\chi^{(2)}$ nonlinearities are more efficient due to parasitic impedances which limit the THz bandwidth of photomixers. Duffy identified several factors which restrict the THz power of cw photomixers including the lifetime of photocarriers, which limits the high THz frequency response, and thermal dissipation, which caps the optical illumination powers and bias voltage levels. For a dual-dipole design, the maximum THz output powers for a single emitter are roughly 3 μW. Arrays of emitters or large gap antennas that produce tens of microwatts of THz power are commercially available.

A recent review of microwave and millimeter wave generation by optical comb techniques can be found in Ref. 63. An optical frequency comb refers to the optical spectrum of a periodic pulse train. Typically the pulse train is generated either by a pulsed mode-locked laser system or by modulation of a continuous laser beam. Ideally, the spectrum consists of a set of discrete frequencies which are separated in frequency by a stable pulse repetition rate. When the optical frequency comb illuminates a high-speed PD detector, the optical signal is rectified producing an electronic output signal within the electronic bandwidth of the PD detector. The electrical output is produced at the frequency interval of the comb and its harmonics. A key feature of the high-speed detector is that it must have an electronic bandwidth in the sub-THz to THz range.

Over the past ten years, the UTC-PD has emerged as a viable high-bandwidth device for optical generation of MMW and sub-THz radiation. UTC-PDs have been developed for both 1.5 μm light using InP/InGaAs (Ref. 64) as well as 800 nm light using GaAs/AlGaAs.[65] The UTC-PD is a heterojunction PD with a p-type absorptive region. An electron-hole pair is generated in the absorption layer when a photon is absorbed. The photogenerated electron moves through a nonlight absorbing collection layer and into the *n*-layer at high velocity. Since the hole carrier moves very slowly in the p-type region due to a diffusion blocking layer, the response of the device—which is in the sub-THz band—is determined by the electron's velocity. Alternative PD structures, such as the separated-transport recombination

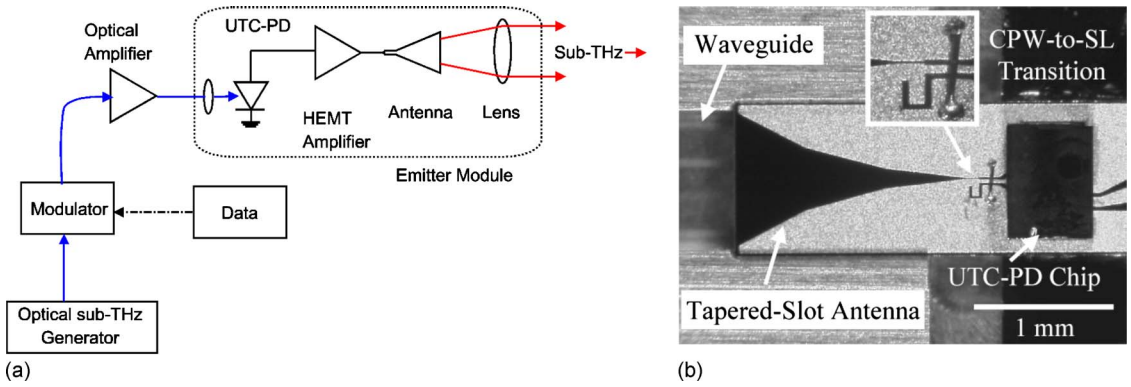

FIG. 9. (Color online) (a) Schematic diagram of sub-THz generation using optical frequency comb in combination with a UTC-PD. Adapted from Ref. 72. (b) Photograph (©2004 IEEE) of core elements of emitter module from Ref. 72, [A. Hirata, T. Kosugi, N. Meisl, T. Shibata, and T. Nagatsuma, "High-directivity photonic emitter using photodiode module integrated with HEMT amplifier for 10-Gbit/s wireless link," IEEE Trans. Microwave Theory Tech. 52, 1843 (2004), (©2004 IEEE)].

PD, have been demonstrated as THz emitters as well.[66] A recent review of high-power radiofrequency and THz PDs can be found in Ref. 67.

Variations in the optical frequency comb technique enable the generation of either multiple sub-THz frequencies or single frequencies. For example, a photomixing geometry can be used. Two single-frequency 1.5 μm lasers beams can be combined, amplified, and then illuminate the UTC-PD to generate tunable THz radiation.[64,67,68] In another embodiment, by splitting the output of an optical comb frequency generator, one then can use injection-locked lasers to each select out a single optical frequency. By combining and amplifying the two selected frequencies, and then illuminating a UTC-PD, power is generated at the difference frequency of the two visible wavelengths corresponding to an integral multiple of the combs frequency interval.[69] Conceptually, the optical frequency comb method of THz generation is equivalent to all-electronic frequency mixing techniques in which the optical frequency comb sources are replace by phase-locked microwave sources which are detuned in frequency to the THz range.[70] The frequency comb is generated by coupling the microwave sources to a nonlinear transmission line pulse generator. The generation of THz radiation by optical frequency combs from two mode-locked Ti:sapphire lasers has also been demonstrated.[71]

Using an optical frequency comb in combination with the UTC-PD, the Microsystem Integration and Photonics Laboratories group at NTT Corporation have demonstrated THz data transmission at ~120 GHz and more recently in the 300–400 GHz band.[68] The photonic sub-THz emitter[72] at 120 GHz consists of an optical comb frequency generator and UTC-PD which converts an optical frequency comb to a sub-THz electrical signal. A schematic of the THz source is shown in Fig. 9. The key features of the source are the optical sub-THz generator (the optical frequency comb) and the photonic emitter. The photonic emitter consists of a UTC-PD which converts modulated optical frequencies in the comb to the sub-THz range, an amplifier, and an antenna structure to launch the sub-THz.

The NTT group has used various methods[67] to generate the optical frequency comb. For example,[27] a 30 GHz reference sine wave can drive a subharmonic mode-locked laser diode (MLLD) to generate an optical pulse train at a repetition rate of 60 GHz. The repetition rate is doubled to 120 GHz by directing the output of the subharmonic MLLD to an optical clock multiplier Mach–Zehnder interferometer device. An alternative method for generating the 120 GHz modulation in the optical pulse train analogous to Ref. 69 is to use beating of two modes from the MLLD in which the two modes are spaced 120 GHz apart. The two modes can be selected using an arrayed waveguide grating. With these methods, one could in principle generate optical combs with frequency spacing at multiples of the 60 GHz repetition rate. In a third variant of the optical frequency comb generator,[73] (Fig. 16) the output of a single-mode laser is modulated at a frequency of 62.5 GHz by a $LiNbO_3$ (LN) optical intensity MZM. The output of the modulator is split into two beams in a planar waveguide coupler. Next, an array waveguide grating selects two of the optical sidebands which are separated in frequency by 125 GHz. These two optical beams are then recombined using a 3 dB coupler. The net output after recombination are two optical beams separated in frequency by 125 GHz. This input can then be amplified by an erbium-doped fiber amplifier (EDFA) and directed into the UTC-PD. For these frequency comb methods to perform satisfactorily, as with all frequency comb methods, a very stable pulse duration is required.[72]

The output of the UTC-PD is amplified by a broad-band high electron-mobility transistor (HEMT) amplifier, while a planar-circuit-to-waveguide substrate transitions the amplified sub-THz signal to an antenna. A high-gain Gaussian optic lens collimates the sub-THz radiation making the photonic emitter highly directional. The HEMT amplifier boosts the sub-THz power that is launched thereby reducing the input optical power necessary for error-free data transmission. With the HEMT amplifier, the photonic sub-THz emitter delivers approximately 8 dBm of 120 GHz power to the launch antenna.[72] Using PD technologies, the maximum output power which has been demonstrated in the 0.4–1 THz range is about 10 μW. Output power levels approaching 1 mW might be possible[67] if (a) the limitations in PD saturation current and dissipation of thermal energy can be circumvented, (b) optimal and efficient coupling between the PD

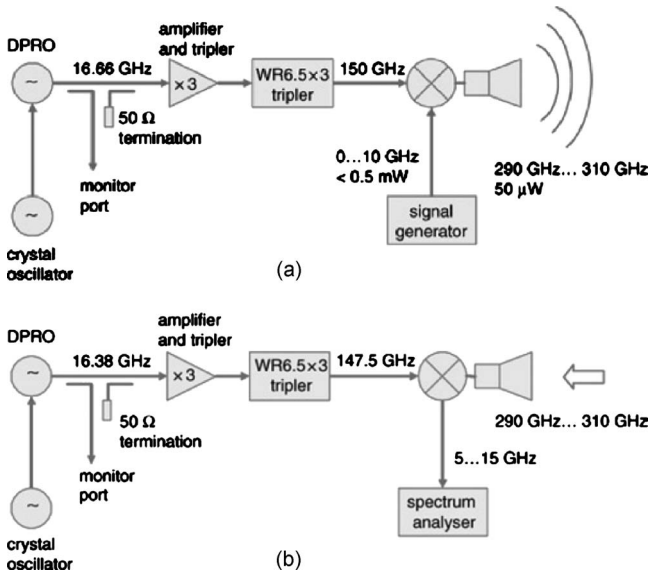

FIG. 10. Microwave frequency multiplier THz source (a) and receiver (b) from Ref. 75 [C. Jastrow, K. Munter, R. Piesiewicz, T. Kurner, M. Koch, and T. Kleine-Ostmann, "300 GHz transmission system," Electron. Lett. 44, 213 (2008), (©IET)].

and launch antenna can be realized, and (c) arrays of antennas can be used to combine the THz power from many PDs into a more powerful THz source.

2. Microwave frequency multipliers

Rather than using optical sources and mixing down the frequency to access the THz range, conceptually one can begin with a lower frequency, i.e., microwave sources and multiply the frequency into the THz range. One method of fabricating microwave frequency multipliers is to use Schottky diode based components.[74] For example, Virginia Diodes has fabricated autarkic (meaning independent or free from external control or constraint) transmitter and receiver units. These transmitter and receiver units (schematic shown in Fig. 10) were used by Jastrow *et al.*[75] to demonstrate the feasibility of THz communications. A 16.66 GHz source consisting of a dielectric phase-locked resonator oscillator with a 10 MHz reference crystal oscillator) is frequency tripled, amplified, and then tripled again. The resulting 150 GHz signal is combined with a local oscillator (LO) from a dc-10 GHz signal generator in a subharmonic mixer. The subharmonic mixer mixes the second harmonic of the 150 GHz input signal with the 0–10 GHz LO signal. Virginia Diode uses a symmetrical diode combination to achieve the mixing with high efficiency. This configuration also requires that the input (150 GHz) and output sub-THz signal frequencies differ by about a factor of 2, so they can be coupled through different waveguides without the need for a diplexer.[76] A feed horn for the sub-THz radiation is directly attached to the mixer block. The authors report that the 50 μW of power is launched at 300 GHz. The newest sources from Virginia diodes produce several milliwatts of power at 300 GHz.

3. Quantum cascade lasers

Since there have been recent reviews[77,78] of THz quantum cascade lasers (QCLs), this review paper will not delve into extensive details but rather on details related to those of THz communication. To date, mid-IR QCLs operate cw at ambient room temperature. The resonant-phonon depopulation scheme has produced good results in the THz: 2.7 THz at 169 K (pulsed) and cw at 3 THz and 117 K. Below 2 THz, the best results are 1.59 THz at 71 K in cw mode. Using a coupling lens, one can obtain 145 mW at 4.1 THz and 160 K. THz QCL are difficult to realize for two reasons[78] such as: (1) Since the THz photons energies are small (~4–20 meV), it is very difficult to inject/remove electrons from closely spaced subbands in order to create the population inversion necessary for gain. (2) Since free-carrier absorption increases as the square of the wavelength of light, the waveguides of QCLs need to minimize the spatial overlap of the lasing modes with the doped semiconducting cladding layers in the waveguides. What is clear from the literature is that THz QCLs operating below 1.5 THz and at room temperature will probably not be available in the near future. In fact, the trend of THz QCLs is that very low temperatures (<40 K) are required to achieve lasing below 1 THz.[78] Based on the frequency dependence of the atmosphere (see Figs. 2 and 4), one would not expect QCLs to play a significant role in wireless THz communication components since the expected frequency of a THz system would be ~300 GHz. One exception to this reasoning could result from frequency mixing (or specifically four wave mixing[22]) of QCLs to generate power in the THz range. Note that limited THz communication demonstrations have been performed with 3.8 THz QCLs.[79]

B. Methods of THz detection for communication links

In studying THz detection methods in the literature, two general trends are clear: (a) some "traditional" THz detectors such as Golay Cells are two slow to respond at the tens of gigabit per second data rates envisioned for a THz communication system (b) the THz detection method is usually intimately linked to the THz generation method. For example, systems in which THz is generated by frequency multiplied microwave sources are typically detected using the same or similar microwave sources. Systems in which the THz is generated optoelectronically, as in THz time-domain or cw photomixing, use the same physical principles as well as laser sources to detect the THz radiation. However, this is not necessarily the case. For example, Loffler *et al.*[80] used a multiplied Gunn emitter as the 0.6 THz source and a mode-locked Ti:sapphire laser in conjunction with a ZnTe crystal for electro-optic detection of the THz radiation. Su *et al.*[81] demonstrated detection of a 94 GHz millimeter wave source using cw THz photomixer detectors. Since THz time-domain and cw optoelectronic photomixing detection have been extensively documented,[82] this section will focus on summarizing other THz detection methods for THz links.

Piesewicz *et al.*[26] suggests Schottky diodes as THz heterodyne mixer detectors. In the most recent results using this concept, Jastrow *et al.*[75] applied a similar design for the mi-

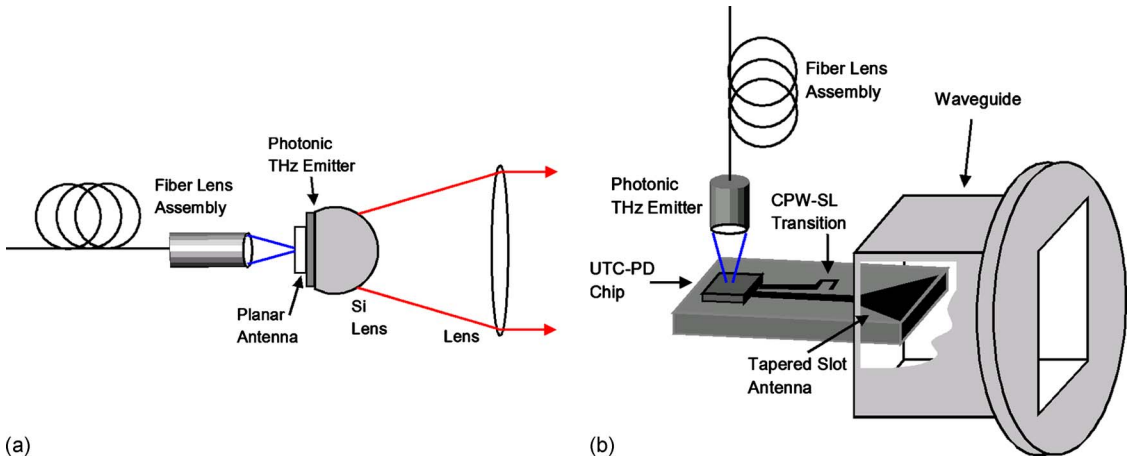

FIG. 11. (Color online) Left: illustration of a planar antenna, silicon lens, and external lens as a sub-THz source. The planar antenna is fabricated on top of a thin layer of high speed photoconductive material. Right: schematic of the waveguide-output photodetector module (adapted from Ref. 72).

crowave multiplier receiver to mix down the incoming THz radiation to a intermediate frequency (IF) of 5 GHz (Fig. 9). Note that on the receiver side, the fundamental microwave oscillator is tuned to 16.38 GHz compared to 16.66 GHz on the transmitter. Consequently, the high frequency signal inputted to the Schottky diode sub-harmonic receiver mixer is 147.5 GHz rather than 150 GHz as in the transmitter. The intermediate frequency from the sub-harmonic mixer is then $2\times(150-147.5)=5$ GHz. The factor of 2 in the calculation results from the fact that the second harmonic of the input is used in the mixing process. While the microwave oscillators for both the transmitter and receiver are freely running independent of each other, their frequencies need to be stabilized such that the IF is fixed.

The experiments by Hirata *et al.*[72] with 120 GHz sub-THz communication systems used a variety of detection systems including Schottky diodes, mixers, and all-electronic InP MMICs.[73,33] The MMIC chipset which is used for the all-electronic transmitters and receivers has an on-wafer measured bit error ratio (BER) of 10^{-12} at 11 Gb/s. It is interesting to note that unlike Jastrow *et al.*'s work in which the THz transmitter and receiver operate on the same physical principles (i.e., Schottky devices), Hirata *et al.* can use their Schottky diode detectors with a variety of THz sources including optical millimeter wave sources (e.g., optical frequency comb/UTC-PD). Since the THz source and MMIC receivers are independent of each other, the receiver unit must include a clock recovery circuit.

C. THz antennas

Koch suggests[22] that planar antenna structures on dielectric lenses and waveguide feed horns are most promising for THz communications. Planar antenna structures can be readily integrated with other planar devices whereas waveguide feed horns have excellent performance and low loss. In the case of the UTC-PD THz source, both antenna types are used. Figure 11(a) illustrates a simple THz source comprised of a planar antenna and silicon lens. (Many standard PDA structure devices (either time-domain or cw photomixing) have a similar construction). The THz radiation interacts with the planar antenna as it is radiated into space. The silicon lens reduces the divergence of the THz radiation from the antenna. An external lens is then used to collimate the light. Figure 11(b) illustrates the coupling of the UTC-PD output first into waveguide structure. The sub-THz signals from the UTC-PD chip are coupled to a tapered slot antenna via a coplanar waveguide. The sub-THz radiation is emitted from the antenna into the rectangular wave guide. The waveguide connects to a feed horn which then couples the radiation to free space.[72]

References 61 and 62 discuss some of the basic science and engineering design considerations of planar antennas and circuitry for cw photomixing antennas. The capacitance of the interdigitated electrodes presents a major challenge in designing high output power antennas. Many of the early photomixers were of the log-spiral type. The advantage of the log-spiral is a large THz bandwidth. The disadvantage is low output power at higher THz frequencies. If one is willing to sacrifice THz bandwidth for improved THz power, then dipole and slot antennas are alternatives. Dual dipole designs, which have the advantage of efficient designs for high-frequency operation, exhibit more symmetric beam patterns and commensurately higher beam-coupling than single element designs. Whereas, dual dipole designs work best at higher frequencies, dual-slot antenna designs are bested suited for high power output <1 THz since it is more difficult to tune out the capacitance of the interdigitated electrodes with the slot design than the dual dipole design. As pointed out by Duffy *et al.*,[61] log-spirals, single, and dual dipoles and slots have limited optical-power handling capability since the electrode region is limited to a fairly small area. The area is limited by (a) partial cancellation of photocurrents due to a phase mismatch across the illuminated active region and (b) the requirement for a small capacitance of the electrode region thereby, enabling inductive tuning. Duffy suggests that a distributed photomixer may improve the bandwidth and output power of photomixers above 1 THz. The company T-Ray Science has introduced arrays of photomixers and transmitters that take advantage of the high optical illumination powers that are available for cw photomixing. Using their photomixing antenna arrays, they demonstrate 1.2 μW microwatts of THz power for 100 mW of

optical input power. Due to the array design, a silicon lens is not required to collimate the THz beam. Their wide aperture (1 mm) antenna can produce ~55 μW of power with 100 mW of optical pumping power. In both of their array and wide aperture designs, they do not observe a saturation in THz power as the optical power is increased.

V. IMPLEMENTATION OF THZ COMMUNICATION

In order to encode a THz carrier with data, clearly some sort of modulation scheme is required. The modulation scheme could either be a direct modulation of a THz source, which is intimately tied to the operational principles of the source, or an external modulator which in principle could be used on a variety of THz sources. In Secs. V A and V B, we briefly review a variety of modulation methods that are applicable to THz communications. First, we treat modulator schemes that are specific to a particular method of THz generation. Second, we review modulator methods that are independent of the particular choice of a THz source. In this review, we consider only modulation schemes that can impress arbitrary data patterns on the THz carrier. In addition to wireless communication, data modulation on THz signals could find application in sensing. When imprinting code sequences on pulse trains, ranging information from far distance scattering objects can be obtained to define selective measurement intervals. This technique is known from M-sequence radar where digital beam modulation enhances the system's unambiguous range.[83,84]

A. THz generator specific modulation schemes

Clearly any modulation methods for THz communication must be capable of encoding THz radiation with random bit patterns in the case of digital data transmission. For both THz time-domain systems as well as cw photomixing systems, one of the standard methods for modulating the THz waveform is a delay line. Most time-domain THz systems use slow mechanical scanning delay lines, or mirror shakers (15–300 Hz repetition rate)[8] to detect the THz waveform on a point by point basis. Following the example of THz TDS, cw photomixing systems (e.g., two laser sources are typically multiplied or mixed in a device such as a PDA structure) typically use a mechanically scanning delay rail[85–87] to vary the optical path of the two IR laser beams after the beams have been combined. The mechanical modulation techniques, however, do not easily permit random delays which would be required for THz data transmission. Improvements to the mechanical modulation methods have included piezoelectric delay lines, which can be modulated with arbitrary voltage waveforms but have limited data rates (kHz).

1. Optoelectronic systems

One method for directly modulating the THz beam from a photoconductive THz antenna is to directly modulate the bias voltage that is applied to the device.[88,89] Since the generated THz is directly proportional to the applied voltage across the photoconductive gap in these devices, a modulation of the applied voltage directly modulates the power of THz radiation with a 100% depth of modulation. Modulation rates of ~1 MHz have been demonstrated with this method.[88] The data rate in these types of modulation experiments, however, is limited to the detection bandwidth of the photoconductive THz detectors to 1MHz.

References 88 and 89 utilize modulation of the THz transmitter bias for time-domain THz communication. An alternative method for modulating cw THz beams, which are generated by the optical mixing of two IR beams in a photoconductive THz antenna, is to modulate the phase (or amplitude) of one of the IR beams.[90] For this method, the phase (or amplitude) of one of the IR beams is modulated at high speeds using a Lithium niobate modulator. Moreover, arbitrary waveforms or bit patterns can be generated by applying the appropriate voltage waveform to the Lithium Niobate modulator. Since the bandwidth of the modulator can be as high as the several gigahertz, one can in principle generate very high bit-rate patterns with this method. The current limitation with this method is the bandwidth of the photoconductive THz receivers.

For cw photomixing, the phase of the THz beam depends on the phase difference of the two IR beams which mix to generate the THz beam. If both beams were phase modulated in unison, there would be no phase shift imposed on the THz beam. Consequently, for the cw photomixer modulation described in Ref. 90, the phase of only one of the IR beams that generates the THz radiation is modulated. The detection of THz by cw photomixers is a phase sensitive measurement: the output of the mixer depends on the relative phase between the incoming THz and the two IR beams which act as a LO for the mixer. Consequently, the signal from the photomixer not only depends on the amplitude of the THz signal but also on the phase of the incoming THz signal which could be altered due to a changing separation between the THz transmitter and receiver. If the phase of the THz beam were unimportant, alternatively one could amplitude modulate one or both of the optical beams. This approach of amplitude modulating the optical beams is used to data encode the optical frequency comb/UTC-PD THz generator (described in Sec. IV A 1). As illustrated in Fig. 16, the optical frequency comb is modulated by data signals via a Lithium Niobate optical modulator and then amplified by a second EDFA.[91]

An alternative method for electronically controlling the phase of a THz beam is through a liquid crystal. While 2π radian phase shifts have been demonstrated, the liquid crystal device necessitates low speed switching operation[92–94] rendering it not useful for the high data rates envisioned for a THz communication system.

2. Schottky diode mixer systems

Mueller and DeMaria[95] proposed a THz modulator based on a sideband-generator which modulates the phase of the radiation upon reflection from a modulated Schottky diode. Essentially, the device acts as an optical delay line whose position can be modulated up to GHz bandwidth. The device requires ~50–100 mW of input THz power and produces a modulated output of 2–4mW.

Improvements to Schottky mixer technology have enabled electronic modulation to THz carrier signals. As illus-

trated in Fig. 10, the modulated data can be introduced through the IF port of the mixer (labeled signal generator in the figure). The modulator method used by Jastrow *et al.*[75] to both modulate and detect the frequency multiplied microwave sources is based on GaAs Schottky barrier diodes[74] as the nonlinear elements in the THz frequency mixers and multipliers. Crowe *et al.* attribute the success of these THz components to three areas of technological innovation:

- The development of advanced fabrication technologies enabling precise fabrication of terahertz diodes and integrated diode circuits.
- The use of advanced computer aided design tools to simulate and optimize both the linear and nonlinear portions of the circuit.
- The development of innovative circuit designs. In particular, the inclusion of planar diodes enables the removal of the whisker-contact which is by far the most difficult and irreproducible part of the component assembly.

Planar diode chips enables the integration of multiple diodes in the circuit design incorporating more complicated circuit designs and higher power throughput. Moreover, the planar diodes enable the circuits to operate over an entire waveguide band eliminating the need for mechanical tuning mechanisms.

B. THz generator independent modulation schemes

Several approaches for external THz modulators have been discussed[96] including ferroelectric materials, liquid crystals,[93,94] and optically or electronically free carriers in semiconductor structures.[97,98] Optically or electrically driven external intensity and phase modulators based on active metamaterials have been demonstrated.[99] However, all of these methods show limited carrier frequency, modulation bandwidth, or modulation index.

Several THz modulators are based on the free-carrier absorption of THz radiation by either optically or electrically injected free carriers. Encoding of data on the THz beam is achieved by controllably modulating the free-carrier concentration in the device. One approach for the direct modulation of THz radiation was demonstrated[97] using an optically controlled mixed type-I/type-II GaAs/AlAs multiple quantum well structure. The long photocarrier lifetimes (0.91 ms) in the structure enables sizeable photoinduced carrier densities for low optical pumping power. When the device is illuminated with visible or near IR light, the increase in free-carrier density results in free carrier absorption of THz radiation which passes through the sample. The device requires low (40 K) temperatures for operation and does not exhibit better than a 72% reduction in THz transmission upon illumination.

Another electronic modulator but one that still required low operating temperatures, utilized five identical parabolic quantum wells with equally spaced electron subbands.[98] An applied electrical field was used to control the electron occupation of the quantum wells and thus the THz free-carrier absorption of the low temperature device. Room temperature operation of an electrically driven THz modulator was achieved by confining a two-dimensional (2D) electron gas at a GaAs/AlGaAs heterointerface.[100] Using fabrication technology for producing high electron mobility transistors, the electron density of the electron gas can be controlled by the application of an external gate voltage. Problematically, the maximum depth of modulation for the device was only 3%. The modulation bandwidth was ~10 kHz.

A silicon waveguide has also been used as a THz modulator. The waveguide is coated with optically transparent films enabling illumination of the waveguide and optical injection of free carriers in the waveguide to modulate THz transmission. The waveguide modulated required 240 mW of average power at 980 nm to achieve 70% modulation.[101] Further improvements to an optically injected free-carrier absorption THz modulator can we achieved by integrating the nonlinear element (e.g., the photodoping region) into a photonic bandgap or metamaterial structure.[96] A photonic bandgap or metamaterial structure—for example, fabricated by alternating layers of high and low refractive index—exhibits spectral bands of high or low photonic transmission. The introduction of a nonlinear layer into the otherwise repetitive structure has two effects such as: (a) introduction of a defect mode by breaking the periodicity of the photonic crystal structure and (b) potentially strong enhancement of the optical nonlinearity of the defect layer due to high localization of the electric field at the defect mode frequency. One structure constructed from alternating layers of crystalline SiO_2 and MgO with a semi-insultating GaAs wafer as a defect layer exhibited a 600 GHz defect band with a FWHM bandwidth of 5–16 GHz. The authors measured the free electron lifetime in the GaAs to be 170 ps. Based on this lifetime, they estimate a maximum switching rate (by optical illumination) to be 5 GHz. They estimate a 50% amplitude modulation corresponding to a 10^{15}–$10^{16}/\mathrm{cm}^3$ concentration of optically induced carriers in a 1 μm thick photoexcited layer. But no experimental results verifying these predictions are presented.

Another example of a photonic bandgap/metamaterial structure for an electronically controllable THz modulator is based on a 2D slit ring resonator (SRR) structure.[102] The measured phase and amplitude of a transmitted THz wave through the structure is shown in Fig. 12. This single layer structure exhibits photonic resonances at 0.81 THz from the individual SRRs and at 1.7 THz from a collective resonance associated with the SRR periodicity. The resonators are fabricated on a 1 μm thick epitaxial layer of *n*-doped GaAs. The SRR and GaAs layer form a Schottky diode structure. The application of a voltage to the diode structure modifies the free carrier concentration in the depletion zone and consequently modifies the tuning of the dielectric properties near the optical bandgaps of the SRRs resulting in a voltage controlled change in the THz transmission. At zero voltage bias the photonic bandgap THz transmission resonances are weak because the intrinsic free carriers shunt the metamaterial's capacitive gaps, leading to relatively small THz absorption at resonance. When a reverse bias voltage is applied to the device, the depletion region increases in size thereby causing an increase in oscillator strength, and THz absorbance, for both resonances.

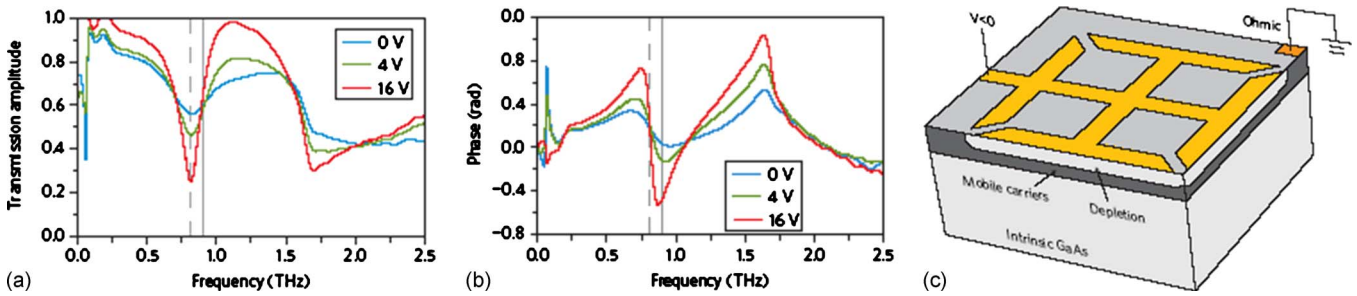

FIG. 12. (Color online) (a) Measured THz transmission amplitude through metamaterial modulator at 0, 4, and 16 V reverse bias. (b) Corresponding phase and (c) structure of single SRR cell of metamaterial illustrating depletion region. Adapted by permission from Macmillan Publishers Ltd: Nature Photonics, Ref. 102, [H. T. Chen, W. J. Padilla, M. J. Cich, A.K. Azad, R. D. Averitt, and A. J. Taylor, " A metamaterial solid-state terahertz phase modulator," Nat. Photonics 3, 148 (2009) (©2009)].

The modulation characteristics of the device are complicated by the fact that the change in transmission amplitude and phase are strongly frequency dependant. If this metamaterial modulator were used for a modulator in a THz communication system, in general *both* the phase and amplitude of the THz signal would be modulated. However, if one operates the device near 0.81 THz, the modulation in phase is minimal while the modulation in amplitude is maximized. Likewise operating the device near 0.89 THz yields maximum phase modulation but minimum amplitude modulation. The maximum transmission intensity change in the device is 80% while the maximum modulation rate is approximately 2 MHz. Until today only simple modulation formats (amplitude modulation) have been demonstrated in THz communication links. But it can be expected that THz communication will follow a similar path to that of radio communication, i.e., more advanced modulation formats as e.g., frequency modulation (FM) or quadrature amplitude modulation will be applied to achieve modulation gain or a higher spectral efficiency. The advantages of such more complex modulation formats are known and the challenges reside on the realization of required modulation hardware.

C. Clock recovery

In several examples for THz communication links in the literature, the same source that is used to drive the emission of THz radiation is also used to detect the THz radiation. For example, in THz time-domain measurements, light from a single mode-locked Ti:sapphire laser is split to drive both the THz transmitting antenna and gate the incoming THz pulses from the receiving antenna. Clearly, in a realistic THz communication link, the THz transmitter and receiver cannot be synchronized by the same source. For the case of a THz link based on time-domain THz, Lin *et al.*[103] suggest using a Piezoelectric-transducer-based optoelectronic phase lock loop to lock two separate Ti:sapphire lasers. This method could be applied to lock the repetition rates of two lasers at transmitting and receiving stations to a remotely distributed clock signal (for example) from a global positioning system.

Clearly, for communications, phase and frequency stability of the THz source relative to the THz receiver is critical. Short time-scale phase and frequency drifts can lead to ISI, amplitude degradation, and timing jitter of the transmitted binary data. Consequently, the phase and frequency stability limits the maximum data rate of the link in the time domain. Additive noise caused by link components or crosstalk will further degrade the link performance. In the cases of THz links based on either THz time-domain or THz cw photomixing, it is the instantaneous THz electric field (not power) that is detected. Consequently, variations in the optical path length between the THz transmitter and receiver must be considered. The path length variations might be due to scintillations, relative motion of the THz transmitter and receiver, or variations in the time duration between THz pulses. Any of these effects will cause a change in the measured instantaneous THz electric field at the detector. Clock tone and phase recovery techniques are needed to compensate for these drifts. While likely clock tone regeneration methods, known from fiber optical communication at multigigabits per second data rates, can be applied on the receiver side, phase recovery for optically triggered receiver will be much more difficult to realize. One way to avoid this problem is the implantation of envelope detection schemes (which is a common approach in radio techniques but has not been demonstrated at THz frequencies so far) or down conversion of the THz carrier to an IF or into baseband where advanced signal processing is suitable to apply. For the later case today's RF synthesizer technology is frequency stable enough to perform this operation which results into a good link performance as demonstrated in Ref. 75.

VI. THZ AND SUB-THZ COMMUNICATION SYSTEMS

In this section, we summarize THz communication experiments to date. As shown in Table I, almost all of the experiments to date have been done in the sub-THz region between 100–300 GHz. A variety of THz sources—THz time-domain, UTC-PD optoelectronic, monolithic microwave integrated circuits (MMICs), and microwave multiplication—were used. The lone exception is a short link (2 m) operating at 3.8 THz using a QCL. Throughout this review paper, the hardware of these systems has been discussed. In this section, we focus on the complete systems as THz communication links.

A. Optoelectonic systems

1. Time-domain systems

The first three examples of THz data communication listed in Table I are based on a THz time-domain system

TABLE I. Summary of THz communication link measurements. BER stands for bit-error-ratio. PDA stands for photoconductive antenna. MZM stands for Mach-Zender modulator.

THz carrier frequency (GHz)	Modulation hardware	Maximum distance (m)	THz system	Modulation method/BW	BER test?	Reference
300	External modulator	0.48	THz time-domain	Analog/external modulator/6 kHz	No	104
300	PDA	1	THz time-domain	Analog/modulate TX bias/5 kb/s	No	89
300	PDA	1	THz time-domain	Digital/modulate TX bias/1 MHz	Yes	88
120	Optical MZM	100	Optical comb/UTC-PD/Schottky diode	Digital/modulation of optical carrier/10 Gb/s	Yes	72
	Lithium niobate	250				73
120	Optical modulator	450	Optical comb/UTC-PD/MMIC receiver	Digital/RoF/10 Gb/s	Yes	28
120	MMIC	800	MMIC	Digital/MMIC/10 Gb/s	Yes	33
250	Optical modulator	0.5	Optical comb/UTC-PD/Schottky diode	Digital/modulation of optical carrier/8 Gb/s	Yes	105
300–400	Optical modulator	0.5	Optical comb/UTC-PD/Schottky diode	Digital/modulation of optical carrier/2 Gb/s	Yes	68
300	Subharmonicmixer	22	Microwave multiplication	Analog/6 MHz	No	75
3800	Electronic	2	QCL	Modulation of pulse generator/Audio bandwidth	No	79

which utilize PDA structures as the THz transmitter and receiver. All three of these examples have some common characteristics:

- The center frequency of the THz pulse is roughly 0.3 THz.
- The absolute maximum possible data rate of the THz time-domain systems is limited by the repetition rate of the Ti:sapphire laser (typically ~80 MHz).
- The electronic bandwidth of the PDA potentially limits the data rate to <1 MHz.
- The transmitter to receiver distance and timing of the gating pulses is adjusted to detect the maximum THz signal detected at the peak of THz pulse. Consequently, timing jitter of the laser or variations in the optical path length degrades the quality of the link.

One of the first demonstrated THz communication links employed a THz time-domain system to transmit analog audio signals[104] on a THz carrier using an external modulator. The transmission distance was 0.48 m. The maximum data rate of the modulator (described in Sec. V A) was ~10 kHz. While audio signals up to 25 kHz could be transmitted, the 3 dB point was ~1 kHz. Reliable data could be transmitted up to about 6 kHz. The bandwidth of the THz detection was limited not only by the time-constant of the lock-in amplifier used to extract the detected signal but also by a 7 kHz cutoff of the I-V amplifier that was used to boost the current signal from the THz detector modules. A schematic of the system is shown in Fig. 13.

Another analog THz link applied LT:GaAs dipole antennas as a THz transmitter and receiver.[89] A Ti:sapphire laser is used to generate and detect THz. Audio signals were impressed upon the THz carrier by directly modulating the bias voltage of the THz transmitter. Reference 89 demonstrated transmission of a six-channel analog and burst audio signal over a distance of 1 m. Peak-to-peak fluctuations of the recorded signal at the receiving antenna over 3 min was about 10% while the signal-to-noise ratio of the detected THz time-domain waveform was around 1000 up to 1 THz. The 3dB frequency response of the transmission channel was about 20 kHz. The photoconductive dipole antennas that were used in the experiment were not designed for high FM. Consequently, the maximum data rate was limited by the RC time constant of the transmitter and receiver. The authors demonstrated transmission of 5 kb/s data bursts. To demonstrate the fidelity of data transmission, they transmitted music through the data channel by using the electronic output from a computer's speaker to modulate the electronic bias to the THz transmitter. In frequency domain, they observed good fidelity of data transmission up to ~2 kHz.

Moeller *et al.*[88] reported bipolar and on/off keying of THz pulses with maximum modulation index by direct data encoding the bias voltage of the photoconductive emitter antenna enabling data rates almost three orders of magnitude higher than described in Refs. 89 and 104. Digital data transmission was characterized by BER measurements. The experimental set-up consisted mainly of a commercially available THz TDS system which is electrically connected to a data source and BER tester (Fig. 14). The THz transmitter (TX) is connected to a pseudorandom bit sequence (PRBS) generator and instead of a constant bias, the emitter antenna is electrically driven by a digital signal carrying the data. A dc-coupled amplifier can increase the voltage at the antenna input to about 20 V. A dc-offset between 0 V and ±Vpp/2 can be added to the pattern generator output, allowing the signal format to vary continuously between bipolar and on/off modulation. As the electrical field of the THz pulse di-

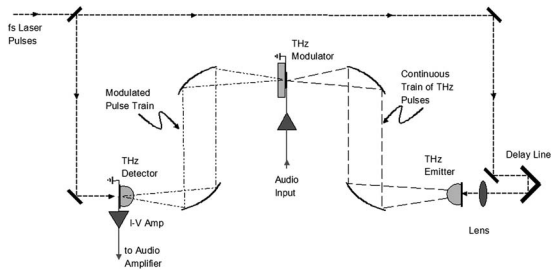

FIG. 13. Experimental setup for analog THz communication link using an external THz modulator (adapted from Ref. 103).

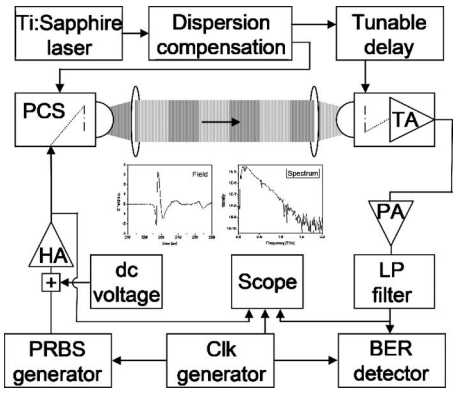

FIG. 14. THz communication set-up based on THz TDS system (Ref. 88). HA high voltage amplifier, PCS photoconductive switch, TA transimpedance amplifier, PA preamplifier, LP low pass, and Clk clock tone from Ref. 88 [L. Möller, J. Federici, A. Sinyukov, C. Xie, H. C. Lim, and R. C. Giles, "Data encoding on terahertz signals for communication and sensing," Opt. Lett. 33, 393 (2008) (©2008)].

rectly depends on the sign and the amount of the applied antenna bias, the PRBS data are linearly mapped onto the THz signal and form its envelope. Sufficient bandwidth of the entire electrical path avoids ISI resulting in rectangular-shaped driving data pulses. The output of the detector antenna is launched via a high gain transimpedance amplifier ($\sim 10^6$ V/A) with ~580 kHz bandwidth into a preamplifier (PA). The PA increases the voltage swing to at least 2 V before passing a low pass filter (LP) with 10 MHz 3dB bandwidth for noise reduction, and finally entering the BER tester's decision gate. Phase-coupled clock tones synchronize the pattern generator and BER tester but oscillate asynchronously relative to the optical pulse train of the modelocked laser. The time delay between the optical pulses that activate the emitter and detector photoconductive switches was adjusted to maximize the electrical receiver output. Impairments due to both electrical ISI (eye closure) and additive noise were observed. The decision gate's threshold and sampling phase is set for a minimum BER.

At error-free operation (BER $< 10^{-8}$) a high impedance sampling scope recorded 0.5, 1, and 1.5 Mb/s eye diagrams [Figs. 15(b)–15(d)] at the PA output, showing the data-rate dependent ISI caused by limited receiver bandwidth. Eye diagrams of bipolar and on/off modulation with the same transmitter voltage swing (TVS) look similar. This is expected since the ac-coupled detector blocks offsets and saturation effects appear to be small at relevant swing levels. At low TVS, receiver noise [Fig. 15(d)] limits the BER = 1×10^{-4} which is manageable using forward error correcting codes.[106] At this BER level we determined the minimal required TVS for different data rates to quantify ISI caused performance degradations [Fig. 15(e)]. A comparison with a second order LP filter simulations of the receiver shows good agreement with the measurement. Increasing the TVS widens the eye which results into a reduced BER. Tests showed that long $(2^{23}-1)$ and short (2^7-1) PRBSs yield same BER performance.

2. Photonic MMW/UTC-PD optoelectronic systems

The NTT group in Japan has been developing sub-THz communication links for the past several years.[67] Over that

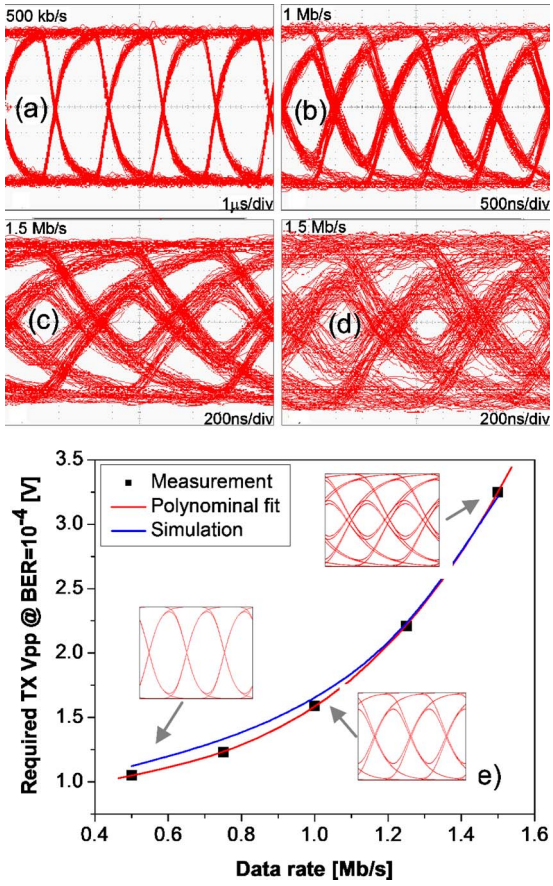

FIG. 15. (Color online) Eye diagrams at different date rates and error-free operation [(a)–(c)] and(d) at 1.5 Mb/s with BER = 10^{-4}; measured and simulated required TVS at different data rates (e). Simulated eye diagrams show good agreement with Figs. 15(a)–15(c) from Ref. 88 [L. Möller, J. Federici, A. Sinyukov, C. Xie, H. C. Lim, and R. C. Giles, "Data encoding on terahertz signals for communication and sensing," Opt. Lett. 33, 393 (2008) (©2008)].

time they have achieved substantial innovations in hardware components. Their contributions listed in Table I focus on three types of systems such as: (a) photonic MMW/UTC-PD sub-THz sources and Schottky diode detectors,[72](b) photonic MMW/UTC-PD sub-THz sources and MMIC receivers,[73] and (c) an integrated MMIC transmitter and receiver.[33] The first two are RoF systems. RoF systems[73] refer to modulating optical carrier signals at millimeter wave frequencies. The optical signals can be routed to a sub-THz transmitter module using low loss optical fibers. Within the THz transmitter module, the modulated optical beam is converted to a sub-THz signal using a UTC-PD and then launched into free-space using a feed horn. The details of the hardware are discussed in Sec. IV A 1. The motivation for the RoF technology as opposed to a conventional millimeter-wave communication link are several fold. One drawback of a conventional wireless millimeter-wave system is that it requires line of sight. While a rooftop to rooftop link would be conceptually straight forward, delivering the MMW signal from the interior of a building, for example, to the roof could be problematic due to attenuating obstacles. Therefore, the available locations for setting up wireless equipment are limited. A RoF system could be a very attractive solution to this problem because the millimeter wave signals can be transmitted

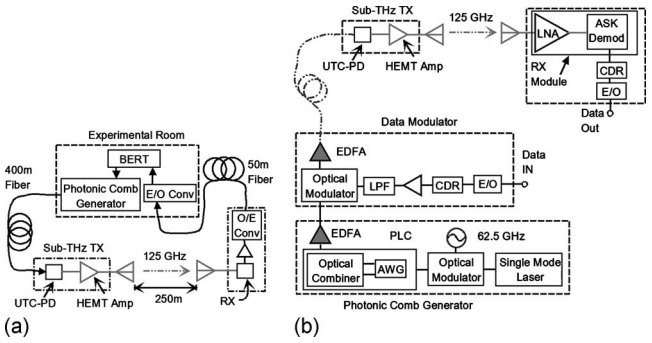

FIG. 16. (a) Schematic of experimental setup for outdoor data communication (adapted from Ref. 73). (b) Details of the various subsystems (adapted from Ref. 73).

over long distances by using optical fibers with an optical frequency comb as discussed in Sec. IV A 1. Conceptually, one can generated the optical frequency comb, encode the data on the optical carrier using an optical modulator, and then route the optical signals through a building to a sub-THz transmitter located on a rooftop. Since a high-gain sub-THz antenna requires highly precise alignment, scintillation effects due to wind or even the motion of buildings will cause variations in the received power. Figure 16 shows a possible configuration for a RoF system which would first transmit optical carriers through a building via fibers, convert the optical comb to wireless sub-THz radiation, and then transform received wireless sub-THz radiation back into infrared light which is then launched back to optical fibers.

Another motivation and advantage of the RoF system is that it can easily be integrated into a high-speed optical fiber communication link as part of a first mile and last mile solution.[27] Conceptually, optical communication systems can provide high-speed (40 Gb/s), long distance point-to-point communication via optical fibers. However, in order to distribute data from a node to the end users, one needs to maintain the high data rate as the data is split among multiple mobile users.

Figure 16 shows a schematic of a RoF wireless link system. The transmitter is composed of a low-phase-noise photonic millimeter-wave generator (described in Sec. IV A 1) which outputs an optical frequency comb: an optical carrier upon which a sub-THz signal is impressed. The output of the photonic millimeter-wave generator passes through the data modulator (described in Sec. V A). At this point, the digital data (which is generated by a bit-error-rate tester) is encoded onto the optical/sub-THz carrier. When the data modulated optical frequency comb illuminates the UTC-PD module, the optical frequency comb is electro-optically converted and amplified by the UTC-PD module to a sub-THz signal. The generated sub-THz signal (with data) is then transmitted from a high-gain antenna. In Hirata's earlier work (see, for example, Ref. 72), the received sub-THz signal can be detected by either a Schottky diode detector or mixer. The Schottky diode detection system exhibited a 10^{-10} BER with a projected maximum distance of 100 m. For the RoF system described in Ref. 73, the received sub-THz signal is detected, amplified, and demodulated by a receiver module using a receiver MMIC chip.[107] The demodulated data signals are then converted to an optical signal by an electro-optic converter and launched into a fiber-optic cable. Finally the optical signal is converted into an electronic signal and launched to a BER tester. A BER below 10^{-12} at 10 Gb/s is reported for a wireless link distance of 250 m. The estimated maximum transmission distance is about 2 km.[28]

B. Integrated circuit systems

While the 1.5 μm fiber-optical components of the RoF systems enable easy integration with high-speed optical communications systems, there is a drawback of the photonic approach in terms of additional optical components, system size, total cost, and added power consumption. Clearly, replacing the optoelectronic THz source with an integrated electronic device—which would work in concert with the MMIC receiver chip—could eliminate many of these issues. Yamaguchi *et al.*[33] implemented a flexible coplanar waveguide MMIC chipset,[108] which included amplifiers, modulators, and demodulators, as the sub-THz transmitter and receiver in a 10 Gb/s wireless link. The link exhibited a 10^{-12} BER over 800 m distance. The authors estimate a maximum transmission distance of 2 km. An interesting note in their paper is that scintillation effects due to the effect of wind on the propagating sub-THz radiation were measurable. As wind velocity increased, the receiver axis deviation also increased which caused the input power to decrease. However, since the input power even in the presence of the wind was greater than the minimum required, the authors did not observe any increase in BER due to the wind.

C. Microwave multiplier systems

Analog video signal transmission has been demonstrated at 300 GHz using a microwave multiplier system.[75] The system, described in Sec. IV A 2), consists of a frequency multiplied (6×) 16.66 GHz LO. The resulting 150 GHz signal is converted to a 290–310 GHz signal using a subharmonic mixer and a dc-10 GHz signal generator. The receiver LO is 16.38 GHz so that the IF of the receiver (5 GHz) is detected using heterodyne methods. To demonstrate data transmission, a color video baseband signal with 6 MHz bandwidth is modulated on a UHF carrier (855.25 MHz) which then acts as the "signal generator" to be transmitted over a THz link. At the receiver, the 5 GHz IF is mixed down to baseband and feed to a standard TV card. The TV card input requires a minimum signal to noise ratio of 40 dB. The image quality is viewed on computer screen. Using just the THz feed horns, excellent picture quality is reported upto 0.5 m with significant degradation observable at transmission distances of 0.8 m. When lenses collimate the THz radiation, a maximum link distance of 22 m is achieved.

VII. SUMMARY AND CONCLUSIONS

THz communication links potentially offer several advantages compared to microwave and IR wireless links including inherently higher bandwidth compared to microwave links and less attenuation under foggy weather or smoke conditions compared to IR links. Moreover, by taking advantage of the wide bandwidth available in the THz range, one can

implement secure communications links in the THz range. While future THz communications links will probably utilize THzIC/MMIC due to their inherently lower-cost compared to optoelectronic systems, near-term systems utilizing frequency multipliers can provide milliwatts of THz power and several gigahertz of bandwidth which should be suitable for reasonable (several hundreds of meters) link distances. Optoelectronic based systems, such as RoF systems, may find niche applications in which direct coupling of wireless THz links to high-speed fiber-optical systems is the major consideration. Several key challenges remain. First and for most is the development of high power THz sources within the THz atmospheric transmission windows, as well as compatible high sensitivity detectors, and modulation hardware. Since one of the potentially major benefits of THz communications is the wide bandwidth, hardware systems that take advantage of the 100 GHz of available bandwidth should be developed over the next several years. Aside from hardware issues, the attenuation and scintillation properties of the atmosphere, including the effect of fog, rain, and smoke, need to be experimentally quantified as THz systems are developed. Lastly, analogous to the development of radio communication, advanced modulation formats need to be applied to the THz links to achieve modulation gain or a higher spectral efficiency.

ACKNOWLEDGMENTS

The authors would like to thank all of our colleagues whose work contributed to this review paper. Technical discussions with S. Personick and C. Xie are gratefully acknowledged.

[1]A. Redo-Sanchez and X.-C. Zhang, IEEE J. Sel. Top. Quantum Electron. **14**, 260 (2008).
[2]M. Tonouchi, Nat. Photonics **1**, 97 (2007).
[3]P. H. Siegel, IEEE Trans. Microwave Theory Tech. **50**, 910 (2002).
[4]P. Mukherjee and B. Gupta, Int. J. Infrared Millim. Waves **29**, 1091 (2008).
[5]G. K. Kitaeva, Laser Phys. Lett. **5**, 559 (2008).
[6]K. L. Vodopyanov, Laser Phys. **19**, 305 (2009).
[7]V. Bratman, M. Glyavin, T. Idehara, Y. Kalynov, A. Luchinin, V. Manuilov, S. Mitsudo, I. Ogawa, T. Saito, Y. Tatematsu, and V. Zapevalov, IEEE Trans. Plasma Sci. **37**, 36 (2009).
[8]W. L. Chan, J. Deibel, and D. M. Mittleman, Rep. Prog. Phys. **70**, 1325 (2007).
[9]R. Appleby and H. B. Wallace, IEEE Trans. Antennas Propag. **55**, 2944 (2007).
[10]M. C. Kemp, 33rd International Conference on Infrared and Millimeter Waves and the 16th International Conference on Terahertz Electronics, IRMMW-THz 2008 (IEEE, New Jersey, 2008).
[11]J. F. Federici, B. Schulkin, F. Huang, D. Gary, R. Barat, F. Oliveira, and D. Zimdars, Semicond. Sci. Technol. **20**, S266 (2005).
[12]J. F. Federici, D. Gary, R. Barat, and Z.-H. Michalopoulou, in *Counter-Terrorism Detection Techniques of Explosives*, edited by J. Yinon (Elsevier, Boston, 2007).
[13]J. A. Zeitler and L. F. Gladden, Eur. J. Pharm. Biopharm. **71**, 2 (2009).
[14]P. H. Siegel, IEEE Trans. Microwave Theory Tech. **52**, 2438 (2004).
[15]Y. L. Hor, J. F. Federici, and R. L. Wample, Appl. Opt. **47**, 72 (2008).
[16]J. F. Federici, R. L. Wample, D. Rodriguez, and S. Mukherjee, Appl. Opt. **48**, 1382 (2009).
[17]D. Zimdars, J. S. White, G. Fichter, G. Sucha, and S. Williamson, in *Ultrasonic and Advanced Methods or Non Destructive Testing and Materials Characterization*, edited by C. H. Chen (World Scientific, Singapore, 2007), Chap. 13, pp. 303–323.
[18]S. K. Reynolds, B. A. Floyd, U. R. Pfeiffer, T. Beukema, J. Grzyb, C. Haymes, B. Gaucher, and M. Soyuer, IEEE J. Solid-State Circuits **41**, 2820 (2006).
[19]R. Heidemann, R. Hofstetter, and H. Schmuck, IEEE MTT-S Int. Microwave Symp. Dig. **1**, 483 (1994).
[20]http://www.fcc.gov/oet/spectrum/.
[21]S. Cherry, IEEE Spectrum **41**, 50 (2004).
[22]M. Koch, *Terahertz Frequency Detection and Identification of Materials and Objects*, Nato Science for Peace and Security Series—B: Physics and Biophysics, edited by R. E. Miles, X. C. Zhang, H. Eisele, and A. Krotkus (Springer Science and Business Media, Dordrecht, Netherlands, 2007), pp. 325–338.
[23]S. Roy, J. Foerster, V. Srinivasa Somayazulu, and D. Leeper, Proc. IEEE **92**, 295 (2004).
[24]Spectrum Management for the 21st Century The President's Spectrum Policy Initiative, Federal Strategic Spectrum Plan, March 2008. http://www.ntia.doc.gov/reports/2008/FederalStrategicSpectrumPlan2008.pdf.
[25]C. M. Mann, "*Towards Terahertz Communications Systems*," Terahertz Sources and Systems, edited by R. Miles *et al.* (Kluwer Academic, Netherlands, 2001), pp. 261–267.
[26]R. Piesiewicz, J. Jemai, M. Koch, and T. Kürner, Proc. SPIE **5727**, 166 (2005).
[27]A. Hirata, M. Harada, and T. Nagatsuma, J. Lightwave Technol. **21**, 2145 (2003).
[28]A. Hirata, T. Nagatsuma, T. Kosugi, H. Takahashi, R. Yamaguchi, N. Shimizu, N. Kukutsu, K. Murata, Y. Kado, H. Ikegawa, H. Nishikawa, and T. Nakayama, Proc. SPIE **6772**, 67720B (2007).
[29]R. Piesiewicz, T. Kleine-Ostmann, N. Krumbholz, D. Mittleman, M. Koch, J. Schoebel, and T. Kurner, IEEE Antennas Propag. Mag. **49**, 24 (2007).
[30]H.-H. Chen, *CDMA Technologies* (Wiley, New York, 2007), Chaps. 2.6.5–2.6.7.
[31]T. Nagatsuma, Talk PL-4 Conference Digest of the 2006 Joint 31st International Conference on IR and MMW, Sept. 18–22, 2006 Shanghai, (China) (IEEE, New Jersey).
[32]http://www.ntia.doc.gov/osmhome/allochrt.pdf.
[33]R. Yamaguchi, A. Hirata, T. Kosugi, H. Takahashi, N. Kukutsu, T. Nagasuma, Y. Kado, H. Ikegawa, H. Nishikawa, and T. Nakayama, RWS 2008, Jan. 22–24, 2008 Orlando, FL (IEEE, New Jersey) p. 695.
[34]V. Jungnickel, T. Haustein, A. Forck, and C. Von Helmolt, Electron. Lett. **37**, 314 (2001).
[35]K.-D. Langer and J. Grubor, Proceedings of 2007 9th International Conference on Transparent Optical Networks, ICTON, July 1–5, 2007 Rome, (IEEE, New Jersey), Vol. 3, pp. 146–151.
[36]N. Cvijetic, D. Qian, and T. Wang, Optical Fiber Conference, 2008 Feb. 24–28, 2008 San Diego (OSA, Washington, DC).
[37]D. Kedar and S. Arnon, IEEE Commun. Mag. **42**, S2 (2004).
[38]K. Wang and D. M. Mittleman, Nature (London) **432**, 376 (2004).
[39]B. Bowden, J. A. Harrington, and O. Mitrofanov, J. Appl. Phys. **104**, 093110 (2008).
[40]J.-K. Lu, C.-P. Yu, H.-C. Chang, H.-W. Chen, and Y.-T. Li, Appl. Phys. Lett. **92**, 064105 (2008).
[41]E. R. Brown, in *Terahertz Sensing Technology*, edited by D. L. Woolard, W. R. Loerop, and M. S. Shur (World Scientific, Singapore, 2003), Vol. 2; Intern. J. High Speed Electron. Systems **13**, 995 (2003).
[42]R. L. Freeman, *Radio System Design for Telecommunications*, 2nd ed. (Wiley, New York, 1997), p. 7.
[43]L. C. Andrews and R. L. Phillips, *Laser Beam Propagation Through Random Media* (SPIE, Bellingham, WA, 1998).
[44]S. A. Khan, A. N. Tawfik, C. J. Gibbins, and B. C. Gremont, IEEE Trans. Antennas Propag. **51**, 3109 (2003).
[45]The original calculation was published in M. J. Rosker and H. B. Wallace, "Imaging through the atmosphere at terahertz frequencies", 2007 IEEE MTT-S International Microwave Symposium Digest, art. no. 4263933, pp. 773–776. Fig. 2 is based on an improved calculation from MMW concepts. www.mmwconcepts.com.
[46]C. F. Bohren and D. R. Huffman, *Absorption and Scattering of Light by Small Particles* (Wiley, New York, 1983).
[47]A. Bandyopadhyay, A. Sengupta, R. B. Barat, D. E. Gary, J. F. Federici, M. Chen, and D. B. Tanner, Int. J. Infrared Millim. Waves **28**, 969 (2007).
[48]B. Wu, B. Marchant, and M. Kavehrad, Military Communications Conference, MILCOM 2007, Oct. 29–31, 2007 Orlando, FL (IEEE, New Jersey), pp. 1–6.
[49]Y. M. Noh, D. Muller, D. H. Shin, H. Lee, J. S. Jung, K. H. Lee, M. Cribb, Z. Li, and Y. J. Kim, Atmos. Environ. **43**, 879 (2009).

[50]H. B. Wallace, (private communication). www.mmwconcepts.com.
[51]H. B. Wallace and C. Xie, (private communication). www.mmwconcepts.com.
[52]R. Piesiewicz, T. Kleine-Ostmann, N. Krumbholz, D. Mittleman, M. Koch, and T. Kürner, Electron. Lett. **41**, 1002 (2005).
[53]S. Wietzke, C. Jansen, and M. Koch, Kunststoffe International **99**, 37 (2009).
[54]D. Turchinovich, A. Kammoun, P. Knobloch, T. Dobbertin, and M. Koch, Appl. Phys. A: Mater. Sci. Process. **74**, 291 (2002).
[55]N. Krumbholz, K. Gerlach, F. Rutz, M. Koch, R. Piesiewicz, T. Kürner, and D. Mittleman, Appl. Phys. Lett. **88**, 202905 (2006).
[56]I. A. Ibraheem, N. Krumbholz, D. Mittleman, and M. Koch, IEEE Microw. Wirel. Compon. Lett. **18**, 67 (2008).
[57]S. Wietzke, C. Jansen, F. Rutz, D. M. Mittleman, and M. Koch, Polym. Test. **26**, 614 (2007).
[58]The company Virginia Diodes (VDI) offers a 300 GHz source based on frequency multiplier chain technology with 30 mW output power.
[59]D. Saeedkia and S. Safavi-Naeini, J. Lightwave Technol. **26**, 2409 (2008).
[60]See, for example, D. Mittleman, in *Sensing with Terahertz Radiation*, edited by D. Mittleman (Springer, New York, 2003).
[61]S. M. Duffy, S. Verghese, and K. A. McIntosh, in *Sensing with Terahertz Radiation*, edited by D. Mittleman (Springer, New York, 2003).
[62]E. R. Brown, in *Terahertz Sensing Technology*, Electronic Devices and Advanced Systems Technology, edited by D. L. Woolard, W. R. Loerop, and M. S. Shur (World Scientific, New Jersey, 2003), Vol. 1.
[63]See collection of papers in T. E. Darcie, A. Stohr, and P. K. L. Yu, J. Lightwave Technol. **26**, 2336 (2008).
[64]H. Ito, Y. Hirota, A. Hirata, T. Nagatsuma, and T. Ishibashi, Electron. Lett. **37**, 1225 (2001).
[65]Y.-T. Li, J. W. Shi, C. Y. Huang, N.-W. Chen, S.-H. Chen, J.-I. Chyi, and C.-L. Pan, IEEE Photon. Technol. Lett. **20**, 1342 (2008).
[66]Y. T. Li, J.-W. Shi, C. Y. Huang, N. W. Chen, S.-H. Chen, J. I. Chyi, Y. C. Wang, C.-S. Yang, and C. L. Pan, IEEE J. Quantum Electron. **46**, 19 (2010).
[67]T. Nagatsuma, H. Ito, and T. Ishibashi, Laser Photonics Rev. **3**, 123 (2009).
[68]T. Nagatsuma, H.-J. Song, Y. Fujimoto, K. Miyake, A. Hirata, K. Ajito, A. Wakatsuki, T. Furuta, N. Kukutsu, and Y. Kado, MWP09—2009 International Topical Meeting on Microwave Photonics, 2009 Oct. 14–26, 2008 Valencia, Spain (IEEE, New Jersey).
[69]S. Fukushima, C. F. C. Silva, Y. Muramoto, and A. J. Seeds, J. Lightwave Technol. **21**, 3043 (2003).
[70]D. W. Van der Weide, J. Murakowski, and F. Keilmann, IEEE Trans. Microwave Theory Tech. **48**, 740 (2000).
[71]T. Yasui, Y. Kabetani, E. Saneyoshi, S. Yokoyama, and T. Araki, Appl. Phys. Lett. **88**, 241104 (2006).
[72]A. Hirata, T. Kosugi, N. Meisl, T. Shibata, and T. Nagatsuma, IEEE Trans. Microwave Theory Tech. **52**, 1843 (2004).
[73]A. Hirata, H. Takahashi, R. Tamaguchi, T. Kosugi, K. Murata, T. Nagatsuma, N. Kukutsu, and Y. Kado, J. Lightwave Technol. **26**, 2338 (2008).
[74]T. W. Crowe, D. W. Porterfield, J. L. Hesler, and W. L. Bishop, Joint 31st International Conference on Infrared Millimeter Waves and 14th International Conference on Terahertz electronics, September 2006 (IEEE, New Jersey, 2006).
[75]C. Jastrow, K. Munter, R. Piesiewicz, T. Kurner, M. Koch, and T. Kleine-Ostmann, Electron. Lett. **44**, 213 (2008).
[76]Tom Crowe, Virginia Diodes (private communication).
[77]S. Kumar and A. W. M. Lee, IEEE J. Sel. Top. Quantum Electron. **14**, 333 (2008).
[78]B. S. Williams, Nat. Photonics **1**, 517 (2007).
[79]P. D. Grant, S. R. Laframboise, R. Dudek, M. Grat, A. Bezinger, and H. C. Liu, Electron. Lett. **45**, 952 (2009).
[80]T. Loeffler, T. May, C. A. Weg, A. Alcin, B. Hils, and H. G. Roskos, Appl. Phys. Lett. **90**, 091111 (2007).
[81]K. Su, Z. Liu, R. Barat, D. Gary, Z.-H. Michalopoulou, and J. F. Federici, Appl. Opt. **49**, E13 (2010).
[82]*Sensing with Terahertz Radiation* D. Mittleman (Springer, New York, 2003).
[83]J. Sachs, P. Peyerl, and M. Rossberg, IEEE Proc. IMTC/99, Venice, Italy, May 24–26, 1999 (IEEE, New Jersey) Vol. 3, pp. 1390–1395.
[84]D. J. Daniels, "*Ground Penetrating Radar*," 2nd ed. (IEE, London, 2004), Chap. 6.6.2.
[85]A. Nahata, J. T. Yardley, and T. F. Heinz, Appl. Phys. Lett. **75**, 2524 (1999).
[86]K. J. Siebert, H. Quast, R. Leonhardt, T. Loffler, M. Thomson, T. Bauer, H. G. Roskos, and S. Czasch, Appl. Phys. Lett. **80**, 3003 (2002).
[87]N. Karpowicz, H. Zhong, J. Xu, K.-I. Lin, J.-S. Hwang, and X.-C. Zhang, Semicond. Sci. Technol. **20**, S293 (2005).
[88]L. Möller, J. Federici, A. Sinyukov, C. Xie, H. C. Lim, and R. C. Giles, Opt. Lett. **33**, 393 (2008).
[89]T.-A. Liu, G.-R. Lin, Y.-C. Chang, and C.-L. Pan, Opt. Express **13**, 10416 (2005).
[90]A. M. Sinyukov, Z. Liu, Y. L. Hor, K. Su, R. B. Barat, D. E. Gary, Z.-H. Michalopoulou, I. Zorych, J. F. Federici, and D. Zimdars, Opt. Lett. **33**, 1593 (2008).
[91]A. Hirata, T. Kosugi, H. Takahashi, R. Yamaguchi, F. Nakajima, T. Furuta, H. Ito, H. Sugahara, Y. Sato, and T. Nagatsuma, IEEE Trans. Microwave Theory Tech. **54**, 1937 (2006).
[92]H.-Y. Wu, C.-F. Hsieh, T.-T. Tang, R.-P. Pan, and C.-L. Pan, IEEE Photon. Technol. Lett. **18**, 1488 (2006).
[93]Z. Ghattan, T. Hasek, R. Wilk, M. Shahabadi, and M. Koch, Opt. Commun. **281**, 4623 (2008).
[94]R. Wilk, N. Vieweg, A. Kopschinski, and M. Koch, Opt. Express **17**, 7377 (2009).
[95]E. R. Mueller and A. J. DeMaria, Proc. SPIE **5727**, 151 (2005).
[96]P. Kužel and F. Kadlec, C. R. Phys. **9**, 197 (2008).
[97]I. H. Libon, S. Baumgartner, M. Hempel, N. E. Hecker, J. Feldmann, M. Koch, and P. Dawson, Appl. Phys. Lett. **76**, 2821 (2000).
[98]R. Kersting, G. Strasser, and K. Unterrainer, Electron. Lett. **36**, 1156 (2000).
[99]H.-T. Chen, W. J. Padilla, J. O. Zide, A. C. Gossard, A. J. Taylor, and R. D. Averitt, Nature (London) **444**, 597 (2006).
[100]T. Kleine-Ostmann, P. Dawson, K. Pierz, G. Hein, and M. Koch, Appl. Phys. Lett. **84**, 3555 (2004).
[101]D. G. Cooke and P. U. Jepsen, Opt. Express **16**, 15123 (2008).
[102]H.-T. Chen, W. J. Padilla, M. J. Cich, A. K. Azad, R. D. Averitt, and A. J. Taylor, Nat. Photonics **3**, 148 (2009).
[103]G. R. Lin, Y. C. Chang, T. A. Liu, and C. L. Pan, Appl. Opt. **42**, 2843 (2003).
[104]T. Kleine-Ostmann, K. Pierz, G. Hein, P. Dawson, and M. Koch, Electron. Lett. **40**, 124 (2004).
[105]H. J. Song, K. Ajito, A. Hirata, A. Wakatsuki, T. Furuta, N. Kukutsu, and T. Nagatsuma, 34th International Conference on Infrared, Millimeter, and Terahertz Waves, IRMMW-THz 2009, Sept. 21–25, 2009 Busan (Korea) (IEEE, New Jersey).
[106]See e.g. International Telecommunications Union standard ITU-T G.975.1 at http://www.itu.int.
[107]T. Kosugi, T. Shibata, T. Enoki, M. Muraguchi, A. Hirata, T. Nagatsuma, and H. Kyuragi, IEEE Int. Microw. Symp. Tech. Dig. **1**, 129 (2003).
[108]T. Kosugi, M. Tokumitsu, T. Enoki, M. Muraguchi, A. Hirata, and T. Nagatsuma, 2004 IEEE CSIC Symp. Dig., Monterey, CA, Oct. 24–27, 2004 (IEEE, New Jersey), pp. 171–174.
[109]N. Cvijetic, D. Qian, J. Yu, Y.-K.Huang, and T. Wang, European Conference on Optical Communication (ECOC) 2009, Sept. 20–24, 2009, Vienna, Austria (IEEE, New Jersey).